BOUNDEDNESS REGIONS OF DISCRETE-TIME DYNAMIC SYSTEMS

Final Report
Contract No. NAS 8-27799
June 30-December 15, 1972

Dragoslav Siljak
Principal Investigator

George J. Thaler
Principal Investigator

Stein Weissenberger
Investigator

The University of Santa Clara • California

This report is prepared for George C. Marshall Space Flight Center, NASA, Marshall Space Flight Center, Huntsville, Alabama 35812 • Date of Publication: March 1, 1972.

CONTENTS

1. Introduction

Many practically important control systems do not have a stable equilibrium. Instead, they may perform satisfactorily while possessing only the kind of behavior characteristic that has been described under various boundedness or practical stability definitions [1]. This report discusses a class of techniques which were developed for obtaining quantitative information about the boundedness properties of such systems. A system of particular interest in this work is the sampled-data control of satellite attitude with quantization. Such a system will be employed throughout as an example of the application of the techniques described.

The report begins with an introduction of various relevant stability concepts as a series of definitions in Section 2; interrelationships are discussed between various definitions in common use. Also included here is a description of the model of a basic sampled-data control system with quantization.

Section 3 describes the basic technique of estimating boundedness regions by means of quadratic Liapunov functions. It also states a sufficient condition, for a certain class of systems, for the existence of a boundedness region. The proof of this condition (Theorem 3-1) involves the estimation technique. Some of the results in this section (Eqn. (3-12) and Eqn. (3-14)) parallel results of Johnson and Lack [2,3], which have also been applied recently by Parker and Hess [4].

Section 4 applies a particular quadratic Liapunov function to the Lur'e-Postnikov class of systems, along the lines proposed by Weissenberger and Siljak [5, 6]. This class of systems is more restricted than that to which the techniques of Section 4 applies; however, the stability property established is the stronger one of absolute boundedness (Definition 4). Relationships are developed for applying the technique to the specific system with quantization.

Section 5 presents an example of the calculation of region-of-boundedness estimates.

Section 6 discusses the linear analysis of the system used in the example and simulation results of the nonlinear system for use in comparison with results obtained in Section 5 by Liapunov techniques.

Section 7 presents conclusions.

The Appendix contains a paper*"On Practical Stability", by Ljubomir Grujić, Visiting Research Associate in the Electrical Engineering Department, University of Santa Clara, on leave from the Mechanical Engineering Department, University of Belgrade, Belgrade, Yugoslavia. This work was motivated by an interest in applying the practical stability concept to the systems of this report, and although it treats only continuous-time systems, useful extensions to discrete-time systems are obvious. Connections between boundedness and practical stability concepts are discussed in Section 2.

*The paper was presented at the Fifth Asilomar Conference on Circuits and Systems, Pacific Grove, California, November 8-10, 1971.

Notation

Throughout this report, except where otherwise noted, lower case Roman letters denote vectors, capital Roman letters denote matrices, lower case Greek letters denote scalars, and capital Greek letters denote sets (except the letter X, which represents the set of all points in the state space). Vectors will be considered as column matrices. The superscript T denotes the transpose and * denotes the conjugate transpose. The notation $H > 0$ means that H is positive definite real symmetric matrix. The letter t is used for discrete-time index, and the letter V for a Liapunov function. The region Ω_c is the complement of Ω.

2. Preliminaries: Definitions and Models

a. Definitions

Consider a discrete-time system described by the equation

$$x_{t+1} = g(t,x_t) + f(t, x_t),\ t = t_o,\ t_o + 1,\ \ldots. \qquad (2\text{-}1)$$

where x_t is the n-vector state of the system and g and f are n-vector functions of time t and state x_t. The vector f is considered as the input to the fundamental, unforced system

$$x_{t+1} = g(t,x_t) \qquad (2\text{-}2)$$

In later applications in this work, a special form will be taken for the function g,

$$g(t,\ x_t) = P\ x_t + q\ \phi(\sigma_t), \sigma_t = r^T x_t\ , \qquad (2\text{-}3)$$

a decomposition into a linear part and a special nonlinear part: P is an n x n matrix of constant coefficients, q is an n-vector of constant coefficients, and ϕ is a scalar function of the linear combination σ of system states. However, for purposes of stating definitions in this section we for the most part retain the more general system description (2-1).

Definition 1

All the motions $x_t(x_o,t_o)$ of system (2-1), are bounded, if for each initial state and time (x_o,t_o) there exists a number $\delta(x_o,t_o) > 0$ such that

$$|x_t(x_o,t_o)| < \delta\ ,\ t \geq t_o\ .$$

The motions of system (2-1) are then said to be Lagrange stable.

By itself, such a boundedness property may give little useful information about the behavior of the system; one quite often

desires at least that all motions ultimately satisfy a particular bound. We are then led to construct

Definition 2

The motions of system (2-1) are said to be ultimately bounded if there exists a number δ such that for each (x_o, t_o) there exists a $t_1 \geq t_o$ such that

$$|x_t(x_o,t_o)| < \delta \ , \ t \geq t_1 \ .$$

Thus, ultimate boundedness implies the existence of a bounded region Ω containing the origin which all solutions ultimately enter.

It is frequently useful to consider a modification of Definition 2 to explicitly recognize this region Ω and also to take into account the fact that for some systems the ultimate boundedness property is not global with respect to initial states: that there are system states from which motions do not enter the region Ω.

Let $\Omega_1 \subset \Omega_2$ be bounded regions containing the origin.

Definition 3

The motions of system (2-1) are said to be ultimately bounded with respect to regions Ω_1 and Ω_2 if for each t_o and for each $x_o \in \Omega_2$ there is a $t_1 \geq t_o$ such that the motion $x_1(x_o,t_o) \in \Omega_1$ for all $t \geq t_1$.

A modification of Definition 3 will find application later to the special system of the form (2-1) - (2-3). Suppose that Φ is a certain class of nonlinear functions $\phi(\sigma_t)$ and that F is a certain class of input functions $f(t, x_t)$. The class Φ will be described later, the class F is the class of bounded inputs,

$$F: \quad |f(t,x_t)| \leq \gamma . \tag{2-4}$$

Definition 4

The motions of system (2-1) - (2-3) are said to be absolutely ultimately bounded with respect to regions Ω_1 and Ω_2, and to the class of nonlinearities Φ and to the class of inputs F, if for each t_o,x, each $x_o \varepsilon\ \Omega_2$,each $\phi \varepsilon \Phi$,and each $f \varepsilon F$,there is a $t_1 > t_o$ such that the motion $x_t(x_o, t_o) \varepsilon\ \Omega_1$ for all $t \geq t_1$.

Closely related to our definitions of boundedness are several notions of practical stability, which were stated originally by LaSalle and Lefschetz, Let $Q_o \subset Q$ be closed and bounded regions containing the origin.

Definition 5

The motions of (2-1) are said to be practically stable if for each $f \varepsilon F$, each t_o, and each $x_o \varepsilon\ Q_o$, the motion $x_t(x_o, t_o) \varepsilon\ Q$ for all $t \geq t_o$. A stronger stability is described by

Definition 6

The motions of (2-1) are said to have strong practical stability if they are practically stable and if in addition for each $f \varepsilon F$, each t_o, and each x_o, there exists a $t_1 > t_o$ such that the motion $x_t(x_o, t_o) \varepsilon\ Q$ for all $t \geq t_1$.

Figure 2-1 illustrates for comparison purposes three divisions of stability behavior: ultimate boundedness with respect to Ω_1, Ω_2, practical stability, and strong practical stability.

Note that the roles of the region of initial conditions (Ω_2, Q_o) and the region in which solutions ultimately enter and remain (Ω_1, Q) are reversed in ultimate boundedness and practical stability: in ultimate boundedness there is a kind of convergence toward a

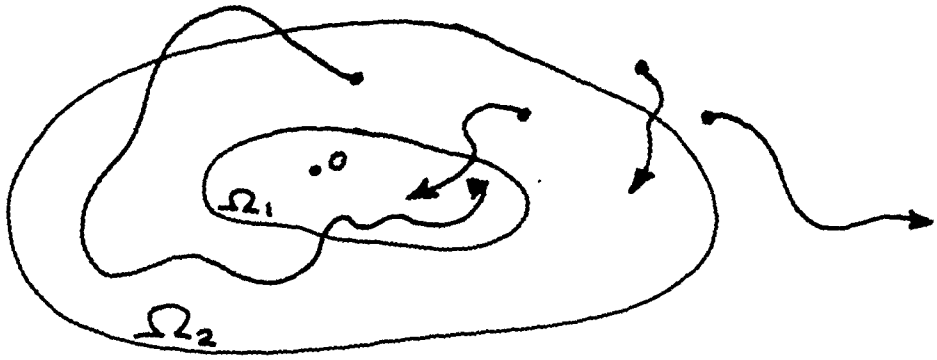

Ultimate Boundedness with Respect to Ω_1, Ω_2

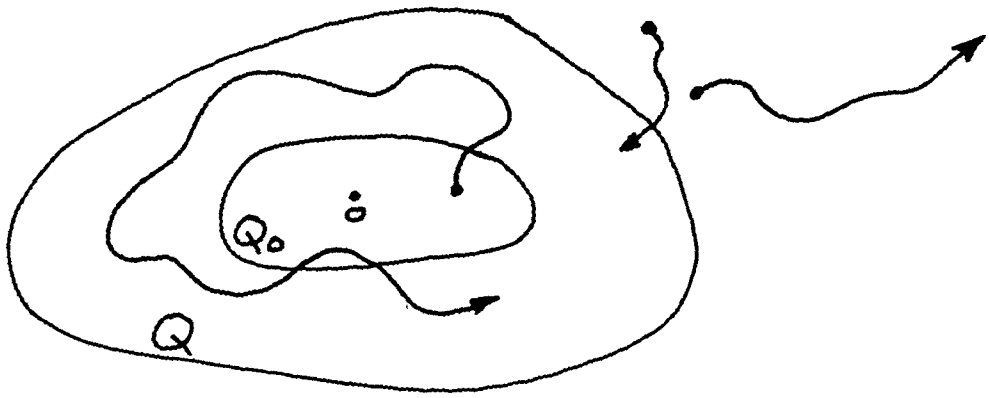

Practical Stability

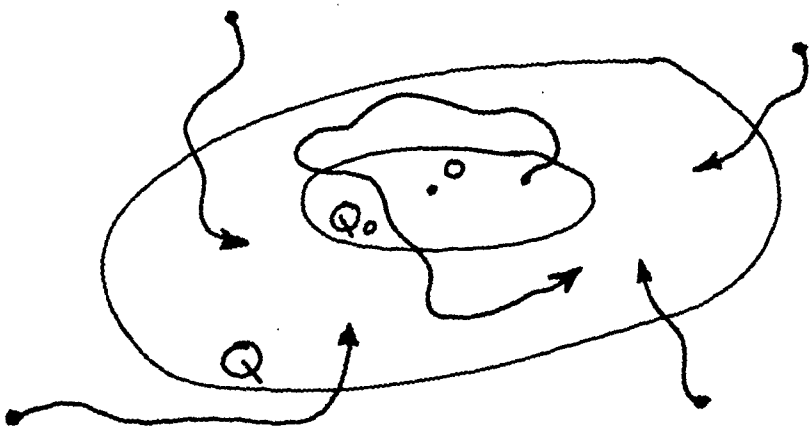

Strong Practical Stability

Note: The indicated behavior holds for each $f \varepsilon F$

FIG. 2-1

COMPARISON OF STABILITY TYPES

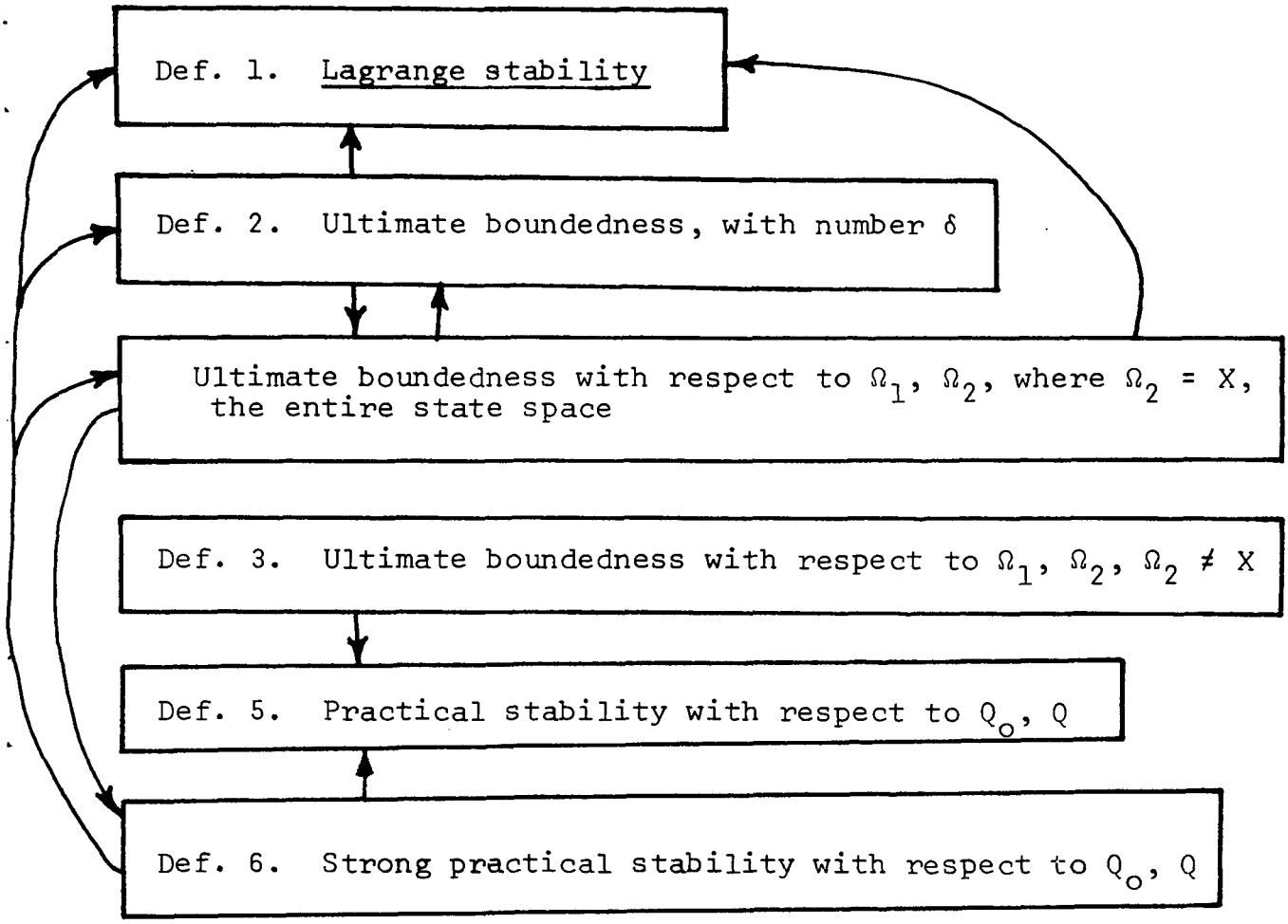

FIG. 2-2

Interrelationships Between Stability Types

neighborhood of the origin in that $\Omega_1 \subset \Omega_2$, while in practical stability, motions are allowed to enter a larger region than the region of initial states, $Q \supset Q_o$. Strong practical stability, however, combines elements of both: there is both practical stability with respect to Q_o, Q and ultimate boundedness with respect to Q, X, where X is the whole state space.

Figure 2-2 shows interrelationships between various stability types. The arrows mean "implies" and are to be understood, for example, in the following sense: ultimate boundedness of motions with respect to certain regions Ω_1, $\Omega_2 (\Omega_2 \neq X)$ implies that there exists some other regions Q_o, Q for which the motions are practically stable.

b. Models

Systems of particular interest in this work are sampled-data control systems containing quantization nonlinearities. The block diagram of a class of such control systems is shown in Fig. 2-3; important features are: linear plant dynamics G(S), time delay T_d, sample and zero-order hold, and a single quantization nonlinearity, which is shown in detail in Fig. 2-4 in a form with saturation.

In subsequent developments, it will be necessary to put system equations in the state-variable form (2-1). Define the discrete-time open-loop transfer function of the system of Fig. 2-3 as

$$G(z) = -\frac{\Sigma(z)}{\Phi(z)} \tag{2-5}$$

where

$$\Sigma(z) = \mathcal{Z}\{\sigma_k\} \tag{2-6}$$

$$\Phi(z) = \mathcal{Z}\{\phi_{ok}[\sigma(k)]\} \tag{2-7}$$

From Fig. 2-3 we calculate

$$G(z) = \mathcal{Z}\{\frac{1-e^{-Ts}}{s} e^{-T_d s} G(s)\} \tag{2-8}$$

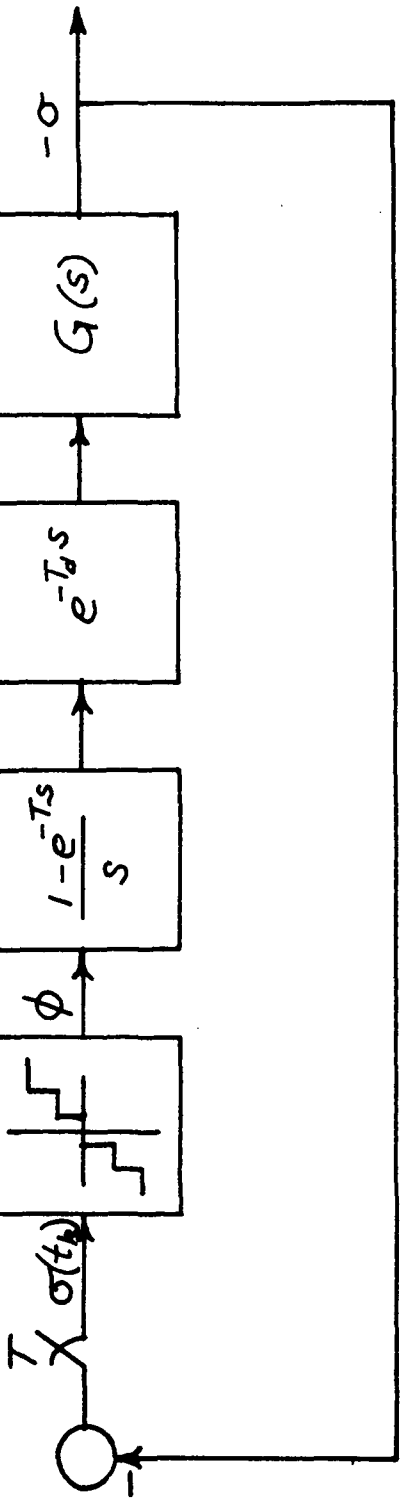

FIGURE 2-3

SAMPLED-DATA CONTROL SYSTEM WITH QUANTIZATION

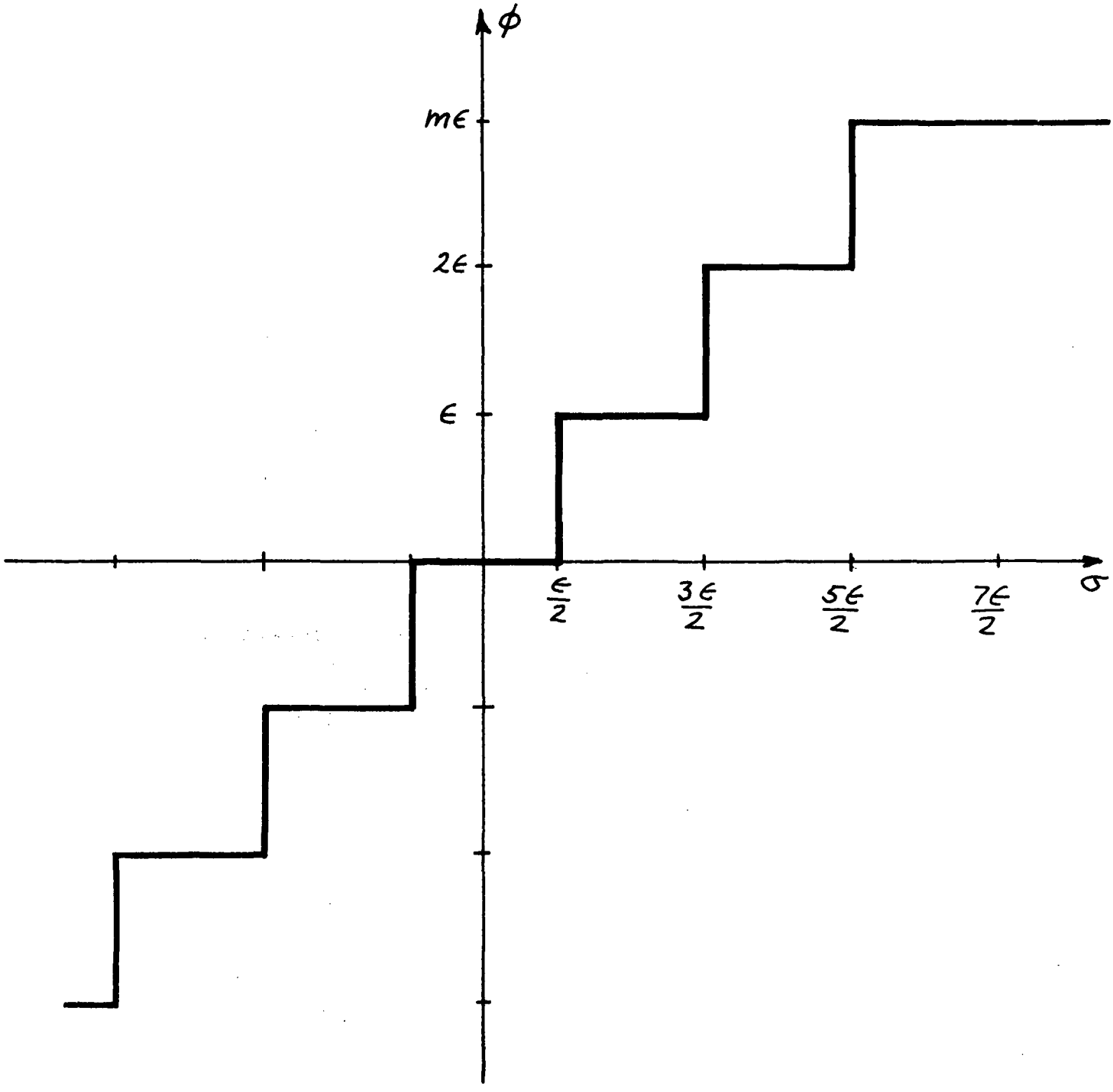

FIGURE 2-4

QUANTIZER NONLINEARITY WITH SATURATION

$$= (1-z^{-1})\,\mathcal{Z}\{e^{-T_d s}\,G(s)\} \tag{2-9}$$

where

$$G_1(s) = \frac{G(s)}{s} \tag{2-10}$$

Then

$$G(z) = (1-z^{-1})\,\mathcal{Z}_m\{G_1(s,m)\}\big|_{m=1-T_d/T} \tag{2-11}$$

where $\mathcal{Z}_m$ is the modified z-transform.

The computation of (2-11) will yield in general,

$$G(z) = \frac{\sum_{i=o}^{n-1} b_i\, z^{i-n}}{1 + \sum_{i=o}^{n-1} a_i\, z^{i-n}}\ ,\ a_i = a_i(m),\ b_i = b_i(m) \tag{2-12}$$

From (2-5) and (2-12) we can construct the state equations

$$x_{t+1} = P\,x_t + q\,\phi\,(\sigma_t) \tag{2-13}$$

$$\sigma_t = r^T x_t$$

where

$$P = \begin{bmatrix} 0 & 1 & \dots & 0 \\ . & 0 & \dots & 0 \\ . & .. & \dots & . \\ 0 & 0 & \dots & 1 \\ -a_o & -a_1 & \dots & -a_{n-1} \end{bmatrix};\ q = \begin{bmatrix} 0 \\ 0 \\ \vdots \\ 0 \\ -1 \end{bmatrix};\ r = \begin{bmatrix} b_o \\ b_1 \\ \vdots \\ . \\ b_{n-1} \end{bmatrix} \tag{2-14}$$

3. Quadratic Liapunov Function Estimates of Boundedness Regions

In this section we establish a sufficient condition for the existence of a region Ω_1 of ultimate boundedness with respect to Ω_1, X. In the process of establishing this condition by means of quadratic Liapunov functions, we formulate techniques for calculating estimates of the region Ω_1.

First, consider the basic

Theorem 3-1: Suppose that the system (2-1) can be put into the form

$$x_{t+1} = Px_t + f(t, x_t) \tag{3-1}$$

where P is a constant coefficient, Hurwitz matrix and the vector f is bounded,

$$f \varepsilon F, \ \forall \ t \geq t_o, \ \forall x.$$

Then there exists a region Ω_1 such that the system (3-1) is ultimately bounded with respect to Ω_1, X.

Proof: Consider the quadratic scalar function

$$V(x) = x^T H x$$

and its difference along motions of (3-1),

$$\Delta V \triangleq V(x_{t+1}) - V(x_t) = (Px_t + f)^T H(Px_t + f) - x_t{}^T H \, x_t$$

$$\Delta V = - x_t{}^T Q x_t + f^T H f \tag{3-2}$$

where $$Q = H - P^T H P, \tag{3-3}$$

Since by assumption

$$|\lambda_i(P)| < 1, \ i = 1,2 \ldots, n,$$

for each $Q > 0$ there exists a unique solution $H > 0$ to Eqn. (3-3) [7]. If $Q > 0$ is chosen, the first term in (3-2) is a positive

definite quadratic form. Since $f \in F$, the second term is bounded. Hence, for sufficiently large $|x|$, $\Delta V < 0$; in this region where $\Delta V < 0$ all motions cross surfaces $V(x)$ = constant from the outside to the inside. Consequently, an estimate $\tilde{\Omega}_1$ of the region Ω_1 will be given by

$$\tilde{\Omega}_1 = \{x: \ V(x) < \tilde{v}_1\} \tag{3-4}$$

$$\tilde{\Omega}_1 \supset \Omega_1 \tag{3-5}$$

where

$$\tilde{v}_1 = \text{maximum } V(x) \quad x: \Delta V(x,t) = 0, \ t \geq t_o. \tag{3-6}$$

Note the <u>conservativeness</u> of the estimate $\tilde{\Omega}_1$ (Eqn. (3-5)). This demonstration has established the theorem and also provided a procedure for calculating estimates $\tilde{\Omega}_1$:

<u>Procedure</u>:

i) Choose $Q > 0$

ii) Determine H from the equation

$$H - P^T H P = Q \tag{3-6}$$

iii) Calculate $\tilde{v}_1$:

$$\tilde{v}_1 = \text{maximum } V(x) \quad x: \Delta V(x,t) = 0, \ t \geq t_o \tag{3-7}$$

i.e., v_1 = maximum $x^T H x$ subject to the constraint

$$-x^T Q x + f(t,x)^T H f(t,x) = 0, \ t \geq t_o$$

iv) $\tilde{\Omega}_1 = x: V(x) < \tilde{v}_1$ (3-8)

In all but contrived, low-order examples, this procedure requires a computer. The calculation of H in (3-5) is straightforward: the equation may be transformed into a set of linear equations in the elements of H, or else various direct algorithms

for the solution of the continuous time version of (3-5) [8] may be employed in conjunction with a bilinear transformation [8]*.

The calculation in step iii) contains the most potential difficulties, depending to some extent on the nature of the function f(t,x). References [9], [10], [11] discuss computer methods which were used successfully in solving the analogous equations which arise in computing quadratic estimates of regions of asymptotic stability for the time-invariant case, $f \equiv f(x)$.

The quality of the approximation, i.e., the "closeness" of $\tilde{\Omega}_1$ to Ω_1 will depend in general on the choice of Q (as well, of course, on one's criterion for evaluating its quality); for each Q a different $\tilde{\Omega}_1$ may be expected to result. A strategy for obtaining improved results would be to determine the elements of Q (subject to the constraint $Q > 0$) which extremize some measure of the quality of Ω_1. The volume is a reasonable quality measure and is readily calculated for a quadratic. The resulting modified procedure is analogous to that used by Weissenberger [12], Nelson [10] and Geiss, et al., [11] to calculate estimates of regions of asymptotic stability.** Its defects are the likelihood of excessive computer time and convergence problems for high-order systems.

Difficulties in the calculation of $\tilde{v}_1$ in (3-7) may be avoided by introducing some degree of approximation and accepting more conservative results. The first term in (3-2) satisfies the inequality

$$- x^T Q x \leq - \lambda_Q |x|^2 \qquad (3\text{-}8)$$

*Let $B = I + 2(P-I)^{-1}$ and $Y = (B^T-I)Q(B-I)$. Solve $B^T H + HB = -\frac{Y}{2}$.

**In the case of boundedness regions, the volume would be minimized, as opposed to the maximization in the case of regions of asymptotic stability.

where $\lambda_Q > 0$ is the minimum eigenvalue of Q. Because $f \varepsilon F$, the second term satisfies the inequality

$$f^T H f > \lambda_h \gamma^2 \tag{3-9}$$

where $\lambda_H > 0$ is the maximum eigenvalue of H.

Eqns. (3-2), (3-8) and (3-9) give

$$\Delta V \leq - \lambda_Q |x|^2 + \lambda_H \gamma^2 \tag{3-10}$$

$$\Delta V < 0$$

for all x such that

$$- \lambda_Q |x|^2 + \lambda_H \gamma^2 < 0$$

or

$$|x| > \gamma \lambda_H^{1/2} \lambda_Q^{-1/2} \triangleq \rho \tag{3-11}$$

Consequently, an estimate $\tilde{\Omega}_1 \subset \Omega_1 \subset \Omega_1$ is given by

$$\tilde{\Omega}_1 = \{x: \ V(x) < \tilde{\nu}_1\} \tag{3-12}$$

where

$$\tilde{\nu}_1 = \underset{|x| = \rho}{\text{maximum}} \ V(x). \tag{3-13}$$

The number $\tilde{\nu}_1$ is readily found to be given by

$$\tilde{\nu}_1 = \lambda_H \rho^2$$

or

$$\tilde{\nu}_1 = \gamma^2 \lambda_H^2 \lambda_Q^{-1} \tag{3-14}$$

In situations where the set of initial states Ω_2 is not the whole state space X, we make use of

Theorem 3-2:

Let $V(x) > 0$, and define the (bounded) regions $\tilde{\Omega}_1$ and $\tilde{\Omega}_2$ as

$$\tilde{\Omega}_1 = \{x: \ V(x) < \tilde{\nu}_1\}$$

and

$$\tilde{\Omega}_2 = \{x: \ V(x) < \tilde{\nu}_2\} \ ,$$

where $0 < \tilde{\nu}_1 < \tilde{\nu}_2$. Assume

$$\tilde{\Omega}_2 / \tilde{\Omega}_1 \quad \{x: \ \Delta V(x) < 0\}$$

Then, the motions of the system (3-1) are ultimately bounded with respect to the regions Ω_1 and Ω_2.

Note that this procedure will produce results which are conservative in the sense that

$$\tilde{\Omega}_1 \supset \Omega_1$$

and

$$\tilde{\Omega}_2 \subset \Omega_2 ,$$

Theorem 3-2 will be employed in Section 4.

4. Lur'e-Postnikov Liapunov Function Estimate of Boundedness Regions

In certain applications, attitude control systems may be modeled by the Lur'e-Postnikov class of systems where the linear part of the system is not asymptotically stable and the quantizer represents the nonlinear characteristic. A simple transformation can be used to make the linear part asymptotically stable which, in turn, forces the quantizer characteristic to violate the usual sector condition in the neighborhood of the origin. An approach to the analysis of this class of systems is to estimate the resulting regions of ultimate boundedness as proposed in references [5] and [6].

The estimation procedure makes use of a quadratic Liapunov function, a modification of the Tsypkin frequency criterion [13], or algebraic test [14], and the Szegö-Kalman construction [15]. In applying the procedure to a specific situation, one has several parameters available with which to improve the estimates of the regions of boundedness.

We consider a free, discrete-time system of the Lur'e class described by the nth-order difference equation,

$$x_{t+1} = P_o x_t + q\, \phi_o(\sigma_t) + f(t,x_t)$$

$$\sigma_t = r^T x_t, \qquad t = 0,1, \ldots \tag{4-1}$$

where x_t, q, and r are real n-vectors; P_o is a real n x n matrix; $\phi_o(\sigma)$ is a real scalar function of the real variable σ, which may have isolated discontinuities; and $f(t,x_t)\ \varepsilon F$. It is assumed that the pair (P_o,q) is completely controllable and the pair (P_o,r^T) is completely observable.

Note that in this section, unlike the previous one, we identify a particular scalar nonlinearity (although we retain also a vector nonlinearity f).

The system (4-1) is transformed into

$$x_{t+1} = Px_t + q\phi(\sigma_t) + f(t,x_t)$$
$$\sigma_t = r^T x_t, \qquad t = 0,1, \ldots \tag{4-2}$$

where

$$P = P_o + \tau q r^T$$
$$\phi(\sigma) = \phi_o(\sigma) - \tau\sigma \tag{4-3}$$

The number τ in (4-3) is chosen in order to insure that the transformed matrix P is Hurwitz, that is, the n eigenvalues $\lambda_k(P)$ of the matrix P satisfy

$$|\lambda_k(P)| < 1, \; k = 1,2, \ldots, n \tag{4-4}$$

and to guarantee that the transformed nonlinear function $\phi(\sigma)$ belongs to the class Φ defined by

$$\Phi: \quad 0 < \sigma\phi(\sigma) < \kappa\sigma^2 \;, \; \alpha_1 \leq |\sigma| \leq \alpha_2$$
$$|\phi(\sigma)| \leq \beta \;, \qquad |\sigma| < \alpha_1 \tag{4-5}$$

where $\alpha_1, \beta \geq 0$, $0 < \alpha_2 \leq +\infty$, and the numbers $\kappa > 0$, $\delta > 0$ are selected to satisfy the inequality

$$\kappa^{-1} + \text{Re } \chi(z) - \delta \, h^* h > 0, \; \forall z: |z| = 1 \tag{4-6}$$

In (4-6),

$$\chi(z) = r^T(P - zI)^{-1} q \tag{4-7}$$

is the open-loop transfer function of the linear part of (4-2) from the input $\phi(\sigma_t)$ to the output $-\sigma_t$, and h(z) is the complex vector defined by

$$h(z) = (P - zI)^{-1} q \tag{4-8}$$

Condition (4-6) is necessary and sufficient [16] for the existence of a function

$$V(x) = x^T H x \tag{4-9}$$

with $H > 0$, such that along the solutions of (4-7)

$$-\Delta V = \delta|x|^2 + (\zeta\phi + P^T x)^2 + \phi(\sigma - \kappa^{-1}\phi) - 2x^T Hf \tag{4-10}$$

where the matrix H, vector P, and scalar ζ satisfy the equations

$$\begin{aligned} H - P^T H P &= PP^T + \delta I \\ q^T H q + \zeta^2 &= \kappa^{-1} \\ P^T H q + q\zeta &= \tfrac{1}{2} r \end{aligned} \tag{4-11}$$

Since the system is described within a Lur'e context, it is natural to use a boundedness property which reflects the class Φ as well as the class F. Such a property was characterized in Section 2 in Definition 4 as absolute boundedness with respect to regions Ω_1 and Ω_2, and classes Φ and F. To calculate estimates $\hat{\Omega}_1$ and $\hat{\Omega}_2$ of the regions Ω_1 and Ω_2 we make use of the function V(x) and Theorem 3-2. Use is also made of the following inequalities, obtained from (4-10):

$$\begin{aligned} -\Delta V &\geq \delta|x|^2 - \lambda_H \gamma |x| - \mu \quad |\sigma| < \alpha \\ -\Delta V &\geq \delta|x|^2 - \lambda_H \gamma |x|, \quad\quad |\sigma| > \alpha \end{aligned} \tag{4-12}$$

where λ_H is the largest eigenvalue of H, and

$$\mu = \beta(\alpha_1 + \kappa^{-1}\beta) \tag{4-13}$$

Based upon inequalities (4-12), the least conservative estimates obtainable for system (4-2) with properties (4-4) and (4-5) are the following:

$$\begin{aligned} \hat{\Omega}_1 &= \{x: V(x) < \hat{\nu}_1\} \\ \hat{\Omega}_2 &= \{x: V(x) < \hat{\nu}_2\} \end{aligned} \tag{4-14}$$

$$\hat{\nu}_1 = \max_{x\in\Lambda_1} x^T H x$$
$$\hat{\nu}_2 = \min_{x\in\Lambda_2} x^T H x \ , \tag{4-15}$$

where

$$\Lambda_1 = \Gamma_1 \cup \Gamma_2 \cup \Gamma_3 \tag{4-16}$$

$$\Gamma_1 = \{x: |x| = \rho_1 \ , \ |r^T x| < \alpha_1\}$$
$$\Gamma_2 = \{x: |x| = \rho_2 \ , \ |r^T x| > \alpha_1\}$$
$$\Gamma_3 = \{x: |r^T x| = \alpha_1, \ \rho_2 \leq |x| \leq \rho_1\} \tag{4-17}$$
$$\rho_1 = \frac{\lambda_H \gamma}{2\delta} + \left[\left(\frac{\lambda_H \gamma}{2\delta}\right)^2 + \frac{\mu}{\delta}\right]^{1/2}$$

$$\rho_2 = \frac{\lambda_H \gamma}{\delta}$$

and

$$\Lambda_2 = \{x: |r^T x| = \alpha_2\} \tag{4-18}$$

An illustration of the sets Λ_1 and Λ_2 in two dimensions is given in Fig. 4-1.

The value of $\hat{\nu}_1$ given in (4-15) can be calculated by the following procedure:

(i) Define

$$\hat{\nu}_{11} = \max_{x\in\hat{\Lambda}_1} x^T H x \ , \tag{4-19}$$

where

$$\hat{\Lambda}_{11} = \{x: |x| = \rho_1\} \tag{4-20}$$

From (4-19) and (4-20), we compute

$$\hat{\nu}_{11} = \lambda_H \rho_1^2 \tag{4-21}$$

Using (4-21) we test

$$\alpha_1 - \hat{\nu}_{11}^{1/2} (\lambda_H e^T e)^{-1/2} r^T e \begin{cases} > 0, \ \hat{\nu}_1 = \hat{\nu}_{11} & \text{(4-22a)} \\ < 0, \text{ go to (ii)} & \text{(4-22b)} \end{cases}$$

where e is an eigenvector corresponding to λ_H.

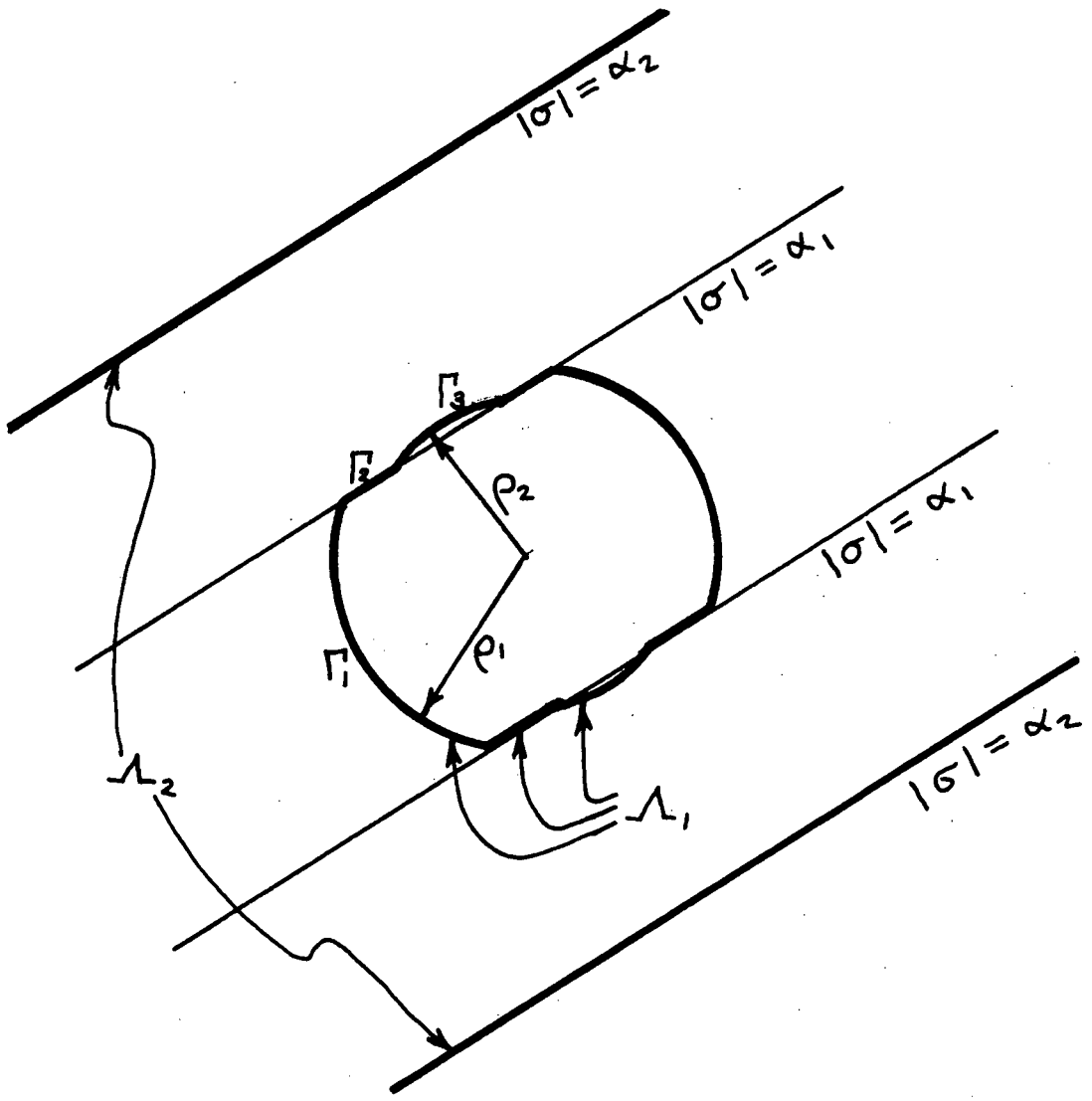

FIGURE 4-1

ILLUSTRATION OF REGIONS Γ_1, Γ_2, Γ_3 AND Ω_1, Ω_2

(ii) Proceeding from (4-22b) we calculate $\hat{\nu}_1$ as follows:

$$\hat{\nu}_{12} = \rho_1^2 \theta_1 + \frac{1}{2} \alpha_1 \theta_2$$

where θ_1 and θ_2 are solutions of the equations

$$\begin{aligned} Hx - \theta_1 \delta x - \tfrac{1}{2} \theta_2 r &= 0 \\ x^T x &= \rho_1^2 \delta^{-1} \\ r^T x &= \alpha_1 \end{aligned} \tag{4-23}$$

Also

$$\hat{\nu}_{13} = \lambda_H \rho_2^2 . \tag{4-24}$$

Then

$$\hat{\nu}_{11} = \max \{\hat{\nu}_{12}, \hat{\nu}_{13}\} . \tag{4-25}$$

Note that the value $\hat{\nu}_{11}$ can always serve as a conservative approximation for $\hat{\nu}_1$.

The value of $\hat{\nu}_2$ given in (4-15) is obtained simply as

$$\hat{\nu}_2 = \alpha_2^2 (r^T H^{-1} r)^{-1} . \tag{4-26}$$

Note that a <u>necessary condition</u> for the existence of estimates $\hat{\Omega}_1 \subset \hat{\Omega}_2$, and a <u>sufficient condition</u> for the existence of regions $\Omega_1 \subset \Omega_2$ is that

$$\hat{\nu}_1 < \hat{\nu}_2 \tag{4-27}$$

It is of interest to point out certain special cases of this analysis that arise when the constraints on nonlinearity α_1 and α_2 assume certain limiting values. If α_1 is reduced to zero the above procedure produces finite regions of absolute stability. When α_2 is infinite the procedure establishes either a global property of absolute ultimate boundedness ($\alpha_1 \neq 0$), or a global property of absolute stability ($\alpha_1 = 0$).

Application to the Quantization Nonlinearity

In order to apply the foregoing analysis technique to the computer control system with quantization described in an earlier section (see Fig. 2.3 and Fig. 2.4), we require calculation of the numbers α_1, α_2, and β. Figure 4-2 shows how these quantities depend on the transformation parameter τ and the Popov sector parameter κ.

Inspection of Fig. 4-2 shows that α_1 is determined by either a lower or upper sector intersection with the transformed nonlinearity,

$$\alpha_1 = \max \{\alpha_L, \alpha_U\}, \tag{4-28}$$

where α_L arises from the intersection with the lower limit of the sector (the σ axis) and α_U arises from the intersection with the upper limit of the sector (the line $\kappa\sigma$). The quantity α_L is obtained from the relations

$$\alpha_L = \left(\frac{2n+1}{2}\right) \varepsilon \tag{4-29}$$

for that integer value of n such that

$$\frac{2n}{2n+1} \leq \tau \leq \frac{2n+2}{2n+3} . \tag{4-30}$$

The quantity α_U is obtained from the relations

$$\alpha_U = \frac{n}{\kappa+\tau} \varepsilon \tag{4-31}$$

for that integer value of n such that

$$\frac{2n-1}{2} \leq \frac{n}{\kappa+\tau} \leq \frac{2n+1}{2} . \tag{4-32}$$

A simpler, conservative estimate of α_1 may be obtained using the straight line envelope of the nonlinearity (the parallel

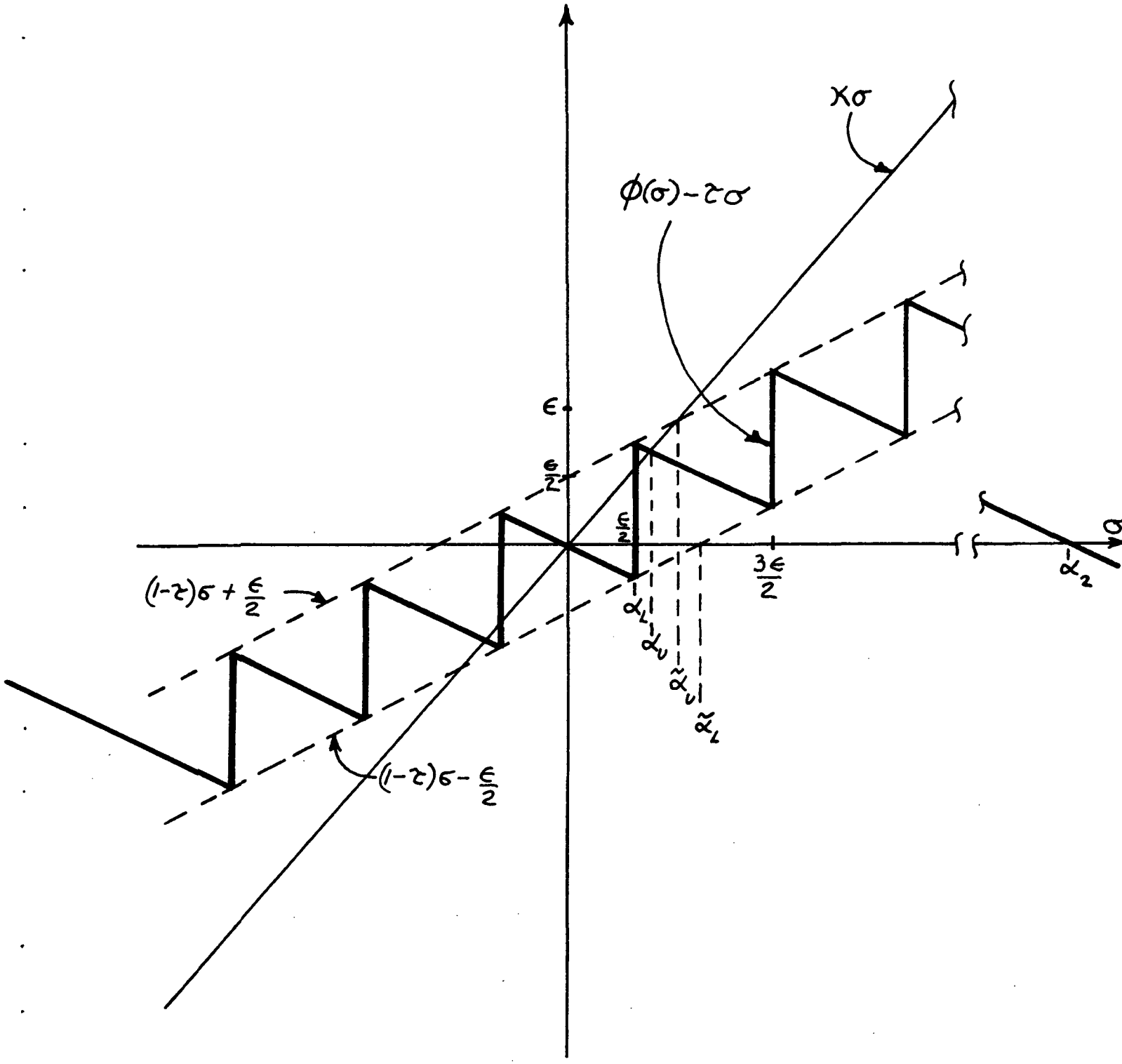

FIGURE 4-2

TRANSFORMED QUANTIZATION NONLINEARITY

dashed lines in Fig. 4-2). We still use (4-28) but in place of (4-29)-(4-32) we have

$$\alpha_L = \tilde{\alpha}_L = \frac{\varepsilon}{2(1-\tau)} \tag{4-33}$$

and

$$\alpha_U = \tilde{\alpha}_U = \frac{\varepsilon}{2(\tau+\tau-1)} \tag{4-34}$$

Since it is necessary that $\alpha_1 > 0$, we have from (4-33) and (4-34) the following limitation on the transformation parameter τ:

$$1-\tau < \tau < 1 \tag{4-35}$$

The approximate analysis from the straight-line envelope also gives, for β,

$$\beta = (1-\tau)\ \alpha_1 + \frac{\varepsilon}{2} \tag{4-36}$$

The value of α_2 is given simply by

$$\alpha_2 = \begin{cases} \dfrac{m + \frac{\varepsilon}{2}}{\tau} & , \quad \tau > 0 \\ + \infty & , \quad \tau \leq 0 \end{cases} \tag{4-37}$$

In those applications, such as satellite attitude control, the linear part of the system is not asymptotically stable, the calculation of regions of absolute ultimate boundedness requires a transformation described in (4-3). Consequently, the first step in the calculation is a selection of τ such that P is Hurwitz and (4-35) is satisfied. To verify (4-35)we need a κ which satisfies frequency condition (4-6) for a certain choice of δ. Once κ and δ are selected, one calculates the vector g by the Szegö-Kalman [15] factorization procedure and computes the matrix H from Eqs. (4-11). After H is determined, one calculates the numbers ν_1 and ν_2 as explained at the end of the preceding section. If either

$\nu_1 > \nu_2$, or estimates Ω_1 and Ω_2 are not satisfactory, one repeats the entire procedure with a different choice of the transformation τ, and possibly different numbers for δ and κ. As is clear from this outline, the application of the proposed method to higher order systems would require utilization of a computer.

5. Example

In this section we perform a numerical calculation of a boundedness region by Liapunov methods. The result will be compared with that to be obtained in Section 6 by simulation. Let the specific system be that to be described subsequently in Section 6 in Fig. 6-7a; this model can be taken as a very simplified representation of a satellite attitude control system. Direct calculation (by integration between sampling intervals) gives the state equations

$$\begin{aligned} x_{t+1} &= P_o\, x_t + q\, \phi_o(\sigma_t) \\ \sigma_t &= r^T x_t \,, \end{aligned} \tag{5-1}$$

where

$$P_o = \begin{bmatrix} 1 & T \\ 0 & 1 \end{bmatrix}$$

$$q^T = -\,[T^2/2 \qquad T]$$

$$r^T = \;[GK_o \qquad GK_1]$$

and ϕ_o is the quantization nonlinearity of Fig. 2-4 with $m = \infty$. The quantity BETA in Fig. 6-7 has been given a unity value, and the quantity GAMMA is denoted above by G.

Using the methods of Section 3 we require a transformation of Eqn. (5-1) to form in which the nonlinearity is bounded. Such a transformation is given by Eqn. (4-3) with $\tau = 1$. Equation (5-1) then becomes

$$\begin{aligned} x_{t+1} &= P\, x_t + q\, \phi(\sigma_t) \\ \sigma_t &= r^T x_t \end{aligned} \tag{5-2}$$

where $P = P_o + q\, r^t$

and $\phi = \phi_o - r^T x$

To calculate a boundedness estimate let us use the simplified form of the calculation which relies on Eqns. (3-6), (3-12), and (3-14):

$$H - P^T H P = Q > 0 \tag{5-3}$$

$$\tilde{\Omega}_1 = \{x: \; V(x) < \tilde{\nu}\} \tag{5-4}$$

$$\tilde{\nu}_1 = \gamma^2 \lambda_H^2 \lambda_Q^{-1} \tag{5-5}$$

where $$V(x) = x^T H x \tag{5-6}$$

The specific choice of numbers in the simulation in Section 6,

$$K_o = 0.292$$

$$K_1 = 1.146$$

$$G = 1.6$$

$$T = 1.0$$

gives

$$P = \begin{bmatrix} 0.76 & 0.08 \\ -0.47 & -0.83 \end{bmatrix}$$

$$q^T = [-0.5 \quad -1.0]$$

$$r^T = [0.467 \quad 1.83]$$

$$\gamma = 0.56\varepsilon$$

Choosing

$$Q = I$$

and solving (5-3), we obtain

$$H = \begin{bmatrix} 2.52 & 0.78 \\ 0.78 & 2.87 \end{bmatrix}$$

Eqn. (5-5) then gives

$$\tilde{\tilde{v}}_1 = 3.8\varepsilon^2$$

so that the estimate of the boundedness region is given by

$$x^T \begin{bmatrix} 2.52 & 0.78 \\ 0.78 & 2.87 \end{bmatrix} x \leq 3.8\varepsilon^2 \qquad (5\text{-}8)$$

This region is shown in Fig. 5-1 together with the region as estimated from the simulation results of Section 6 in Figs. (6-13) through (6-15). The overlap of the regions may be due to inaccuracies in estimation from the simulation results: the actual region may be smaller than was concluded from the simulation, due to the very complex, long-duration dynamic behavior of the simulated system. In any case, more examples and comparisons are needed before a definitive statement can be made about the merits of the Liapunov approach.

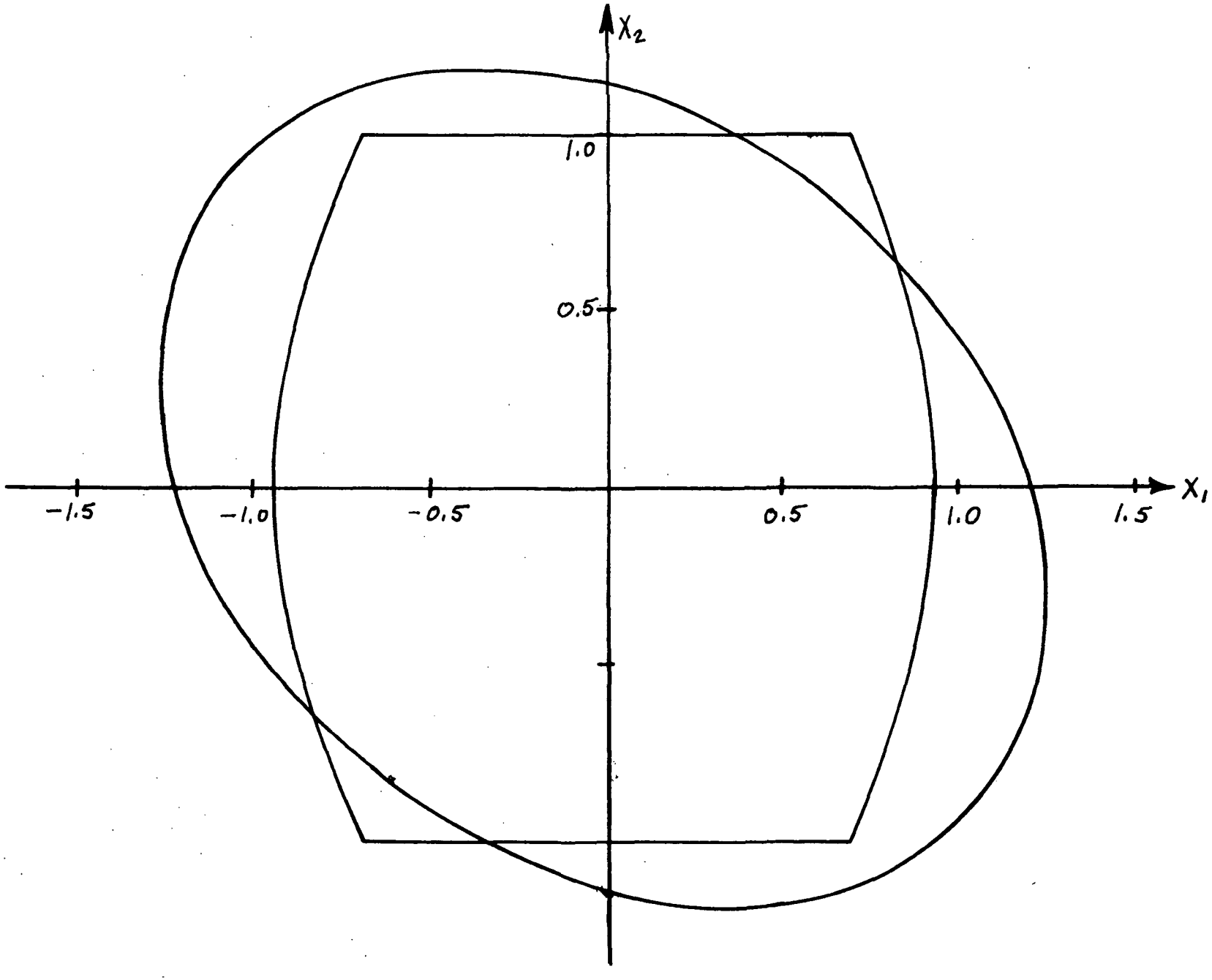

FIG. 5-1

ESTIMATION OF BOUNDEDNESS REGION VIA LIAPUNOV FUNCTION AND SIMULATION

6. Linear Analysis and Simulation Results

a. Linear Sampled Data Studies

One model of an attitude control for a satellite has been given by Seltzer [17] and is represented in Fig. 6-1 as Model A. An alternate representation representing somewhat different instrumentation is given in Fig. 6-1 as Model B. Both models are linear sampled data systems with digital compensator and a time delay due to the use of the digital computer. It is intended that a nonlinearity (a quantizer) be inserted into Model B, and the effect of such nonlinearity on stability is to be studied. First, however, a linear analysis of Model B is undertaken with appropriate comparisons to Model A.

Symbol equivalences in the two models:

Model A	Model B
K_0	K_p
K_1	K_v
K_2	K_a
1	K
$k_0 = K_0T^2/2I$	$k_0 = KK_0T^2/2I$
$k_1 = K_1T/I$	$k_1 = KK_vT/I$

In Z-domain, the characteristic equations and transfer functions for Model A (with digital filter and $F(Z) = \frac{Z}{Z+K_2}$) and Model B (without digital computer) are as follows:

Model A

Characteristic Equation:

$$Z^3 + (K_2 - 2)Z^2 + (1 + k_0 + k_1 - 2K_2)Z + (k_0 - k_1 + K_2) = 0$$

MODEL A (Seltzer's model)

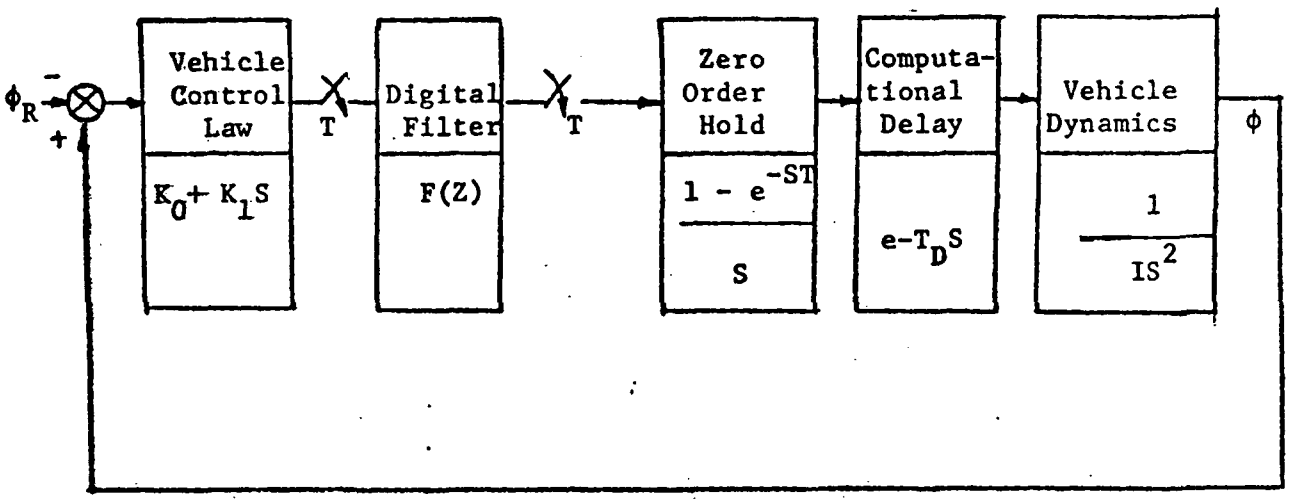

MODEL B

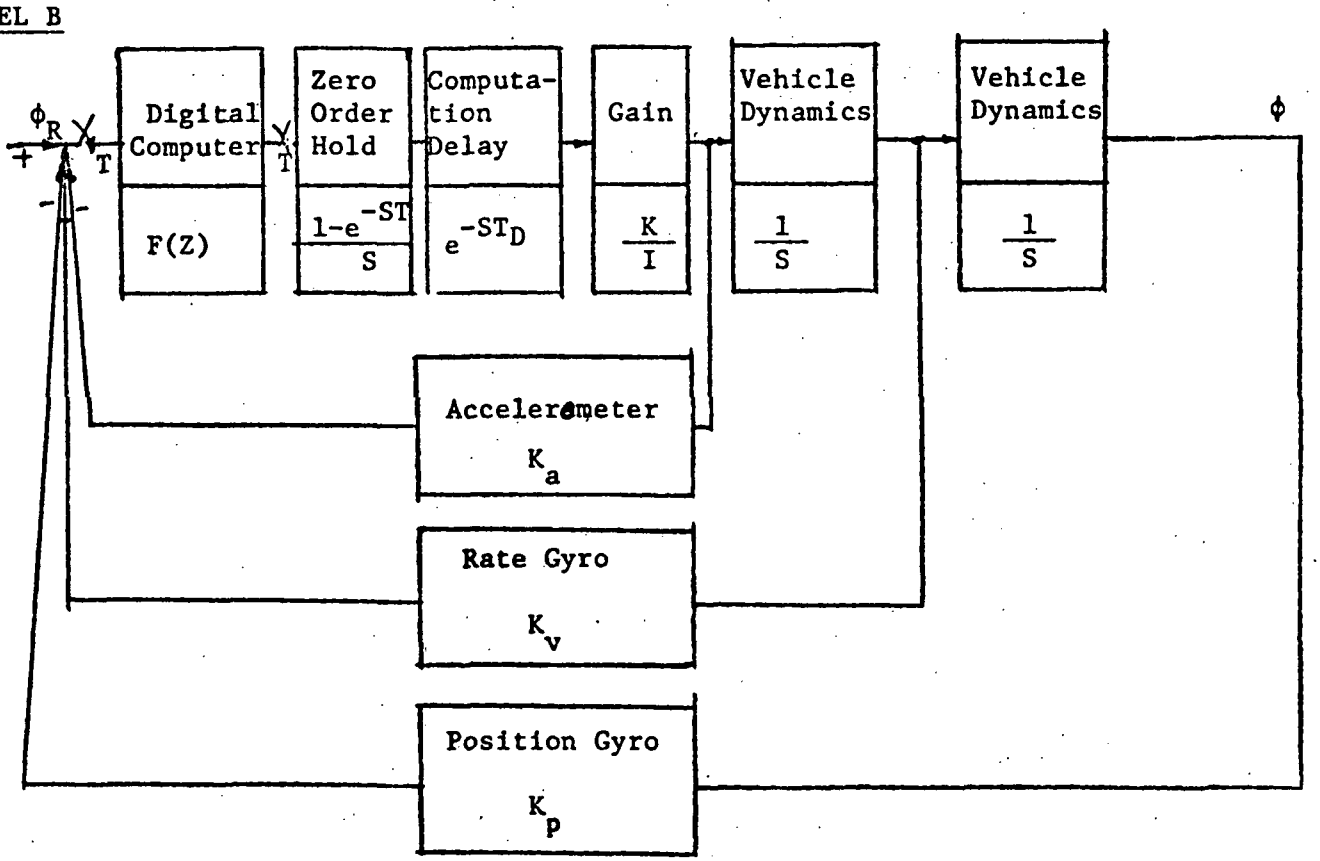

FIG. 6.1: TWO MODELS FOR A LINEAR SYSTEM

Transfer Function:

$$\frac{\phi}{\phi_R} = \frac{(k_0 + k_1)Z + (k_0 - k_1)}{Z^3 + (K_2 - 2)Z^2 + (1 + k_0 + k_1 - 2K_2)Z + (k_0 - k_1 + K_2)}$$

or:

$$\frac{\phi}{\phi_R} = \frac{(k_0 + k_1)Z^{-2} + (k_0 - k_1)Z^{-3}}{1 + (K_2 - 2)Z^{-1} + (1 + k_0 + k_1 - 2K_2)Z^{-2} + (k_0 - k_1 + K_2)Z^{-3}}$$

Model B

Characteristic Equation:

$$Z^3 + (K_2 - 2)Z^2 + (1 + k_0 + k_1 - 2K_2)Z + (k_0 - k_1 + k_2) = 0$$

Transfer Function:

$$\frac{\phi}{\phi_R} = \frac{(0.5)KT^2(Z + 1)}{Z^3 + K_2 - 2)Z^2 + (1 + k_0 + k_1 - 2K_2)Z + (k_0 - k_1 + K_2)}$$

or (set K = 1)

$$\frac{\phi}{\phi_R} = \frac{(0.5)T^2(Z^{-2} + Z^{-3})}{1 + (K_2 - 2)Z^{-1} + (1 + k_0 + k_1 - 2K_2)Z^{-2} + (k_0 - k_1 + K_2)Z^{-3}}$$

Notice that both Model A and Model B have identical characteristic equations.

In Z-domain, the stability boundary is the unit circle, i.e., $|Z| = R = 1$.

Stability: $|Z| < 1$

Instability: $|Z| > 1$

Z-plane

$$Z = e^{ST} = RE^{i\theta}$$

$$R = e^{-\zeta W_n T} \quad , \quad \theta = W_n T(1-\zeta^2)^{1/2}$$

where ζ = damping ratio

W_n = natural frequency

T = sampling period

The stability contours (for complex boundaries) of K_2 (third parameter) in parameter k_0 - k_1 plane are as shown in Fig. 6-2. This corresponds to Seltzer's Fig. 4-1, but is explicit, i.e., it has been computed quantitatively for a number of values of K_2. The plot is done by a digital computer by introducing Chebyshev functions into the characteristic equation. One real root boundary, Z = 1, is k_0 = 1 (i.e., K_2 - k_1 plane); it is independent of the values of K_2 and K_1 in 3-D space. Another (Z = - 1) is calculated by setting Z = - 1 in the characteristic equation, and it is a plane defined by the equation $k_1 = 2(K_2 - 1)$ in the 3-D space which we can see is independent of k_0. 3-D space is not easy to show. However, in the parameter plane (2-D) for K_2 = 1, the stable region is bounded by the two axes and the complex boundary as depicted in Fig. 6-2. Relative stability contours in the parameter plane K_2 = 0, K_2 = 0.5, K_2 = 1, K_2 = 2 are computer plotted, shown in Figs. 6-3,4,5 and 6, respectively, for discrete varying values of R and θ, again Chebyshev functions are introduced into the characteristic equation for the computer program. Figures 6-3, 5, and 6 correspond to Seltzer's Figs. 5, 6 and 7, respectively, the only difference being in the variables chosen for mapping.

The correlations of the above-mentioned graphs and those of Figs. 5, 6, and 7 of Seltzer's paper are developed as follows:

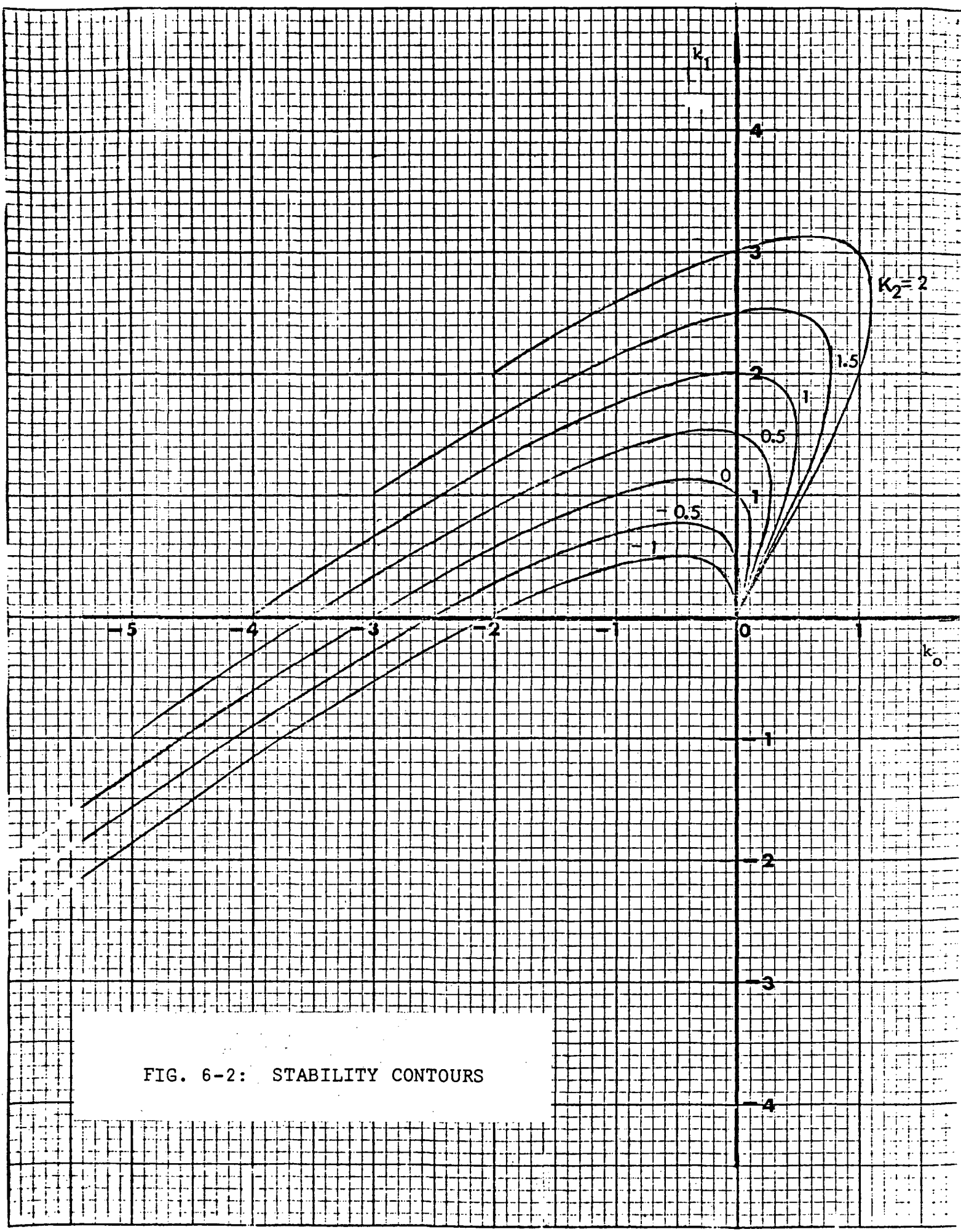

FIG. 6-2: STABILITY CONTOURS

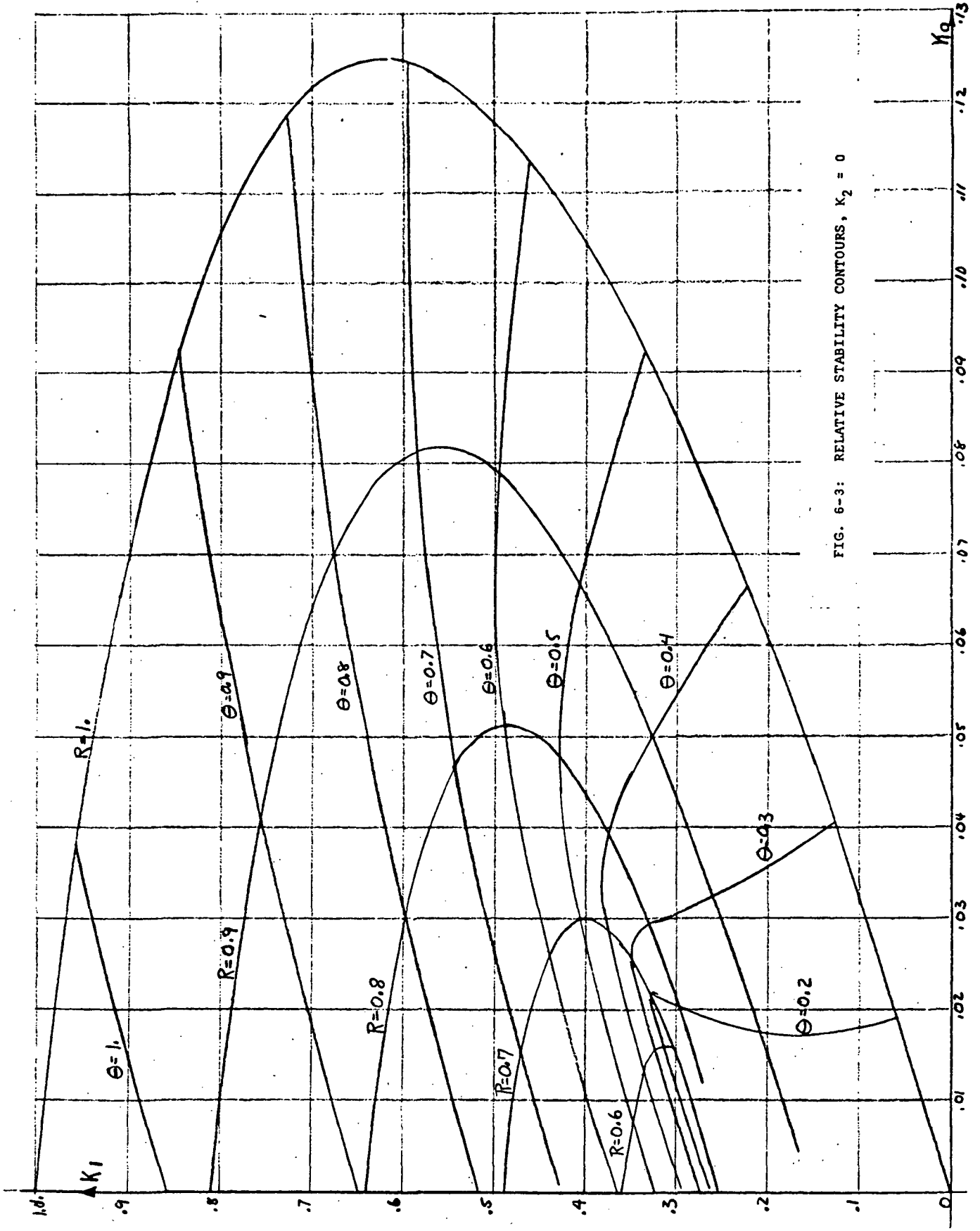

FIG. 6-3: RELATIVE STABILITY CONTOURS, $K_2 = 0$

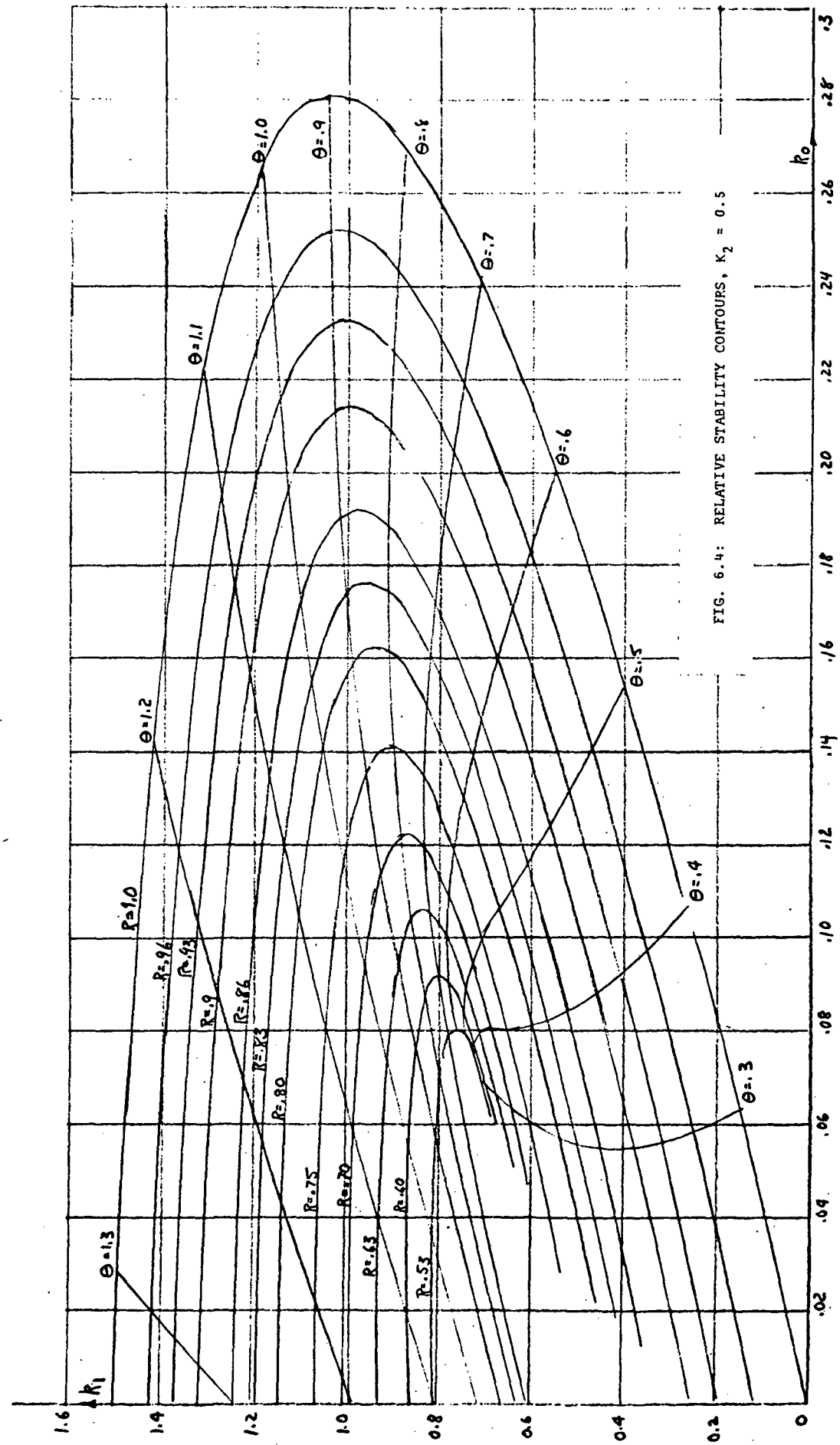

FIG. 6.4: RELATIVE STABILITY CONTOURS, $K_2 = 0.5$

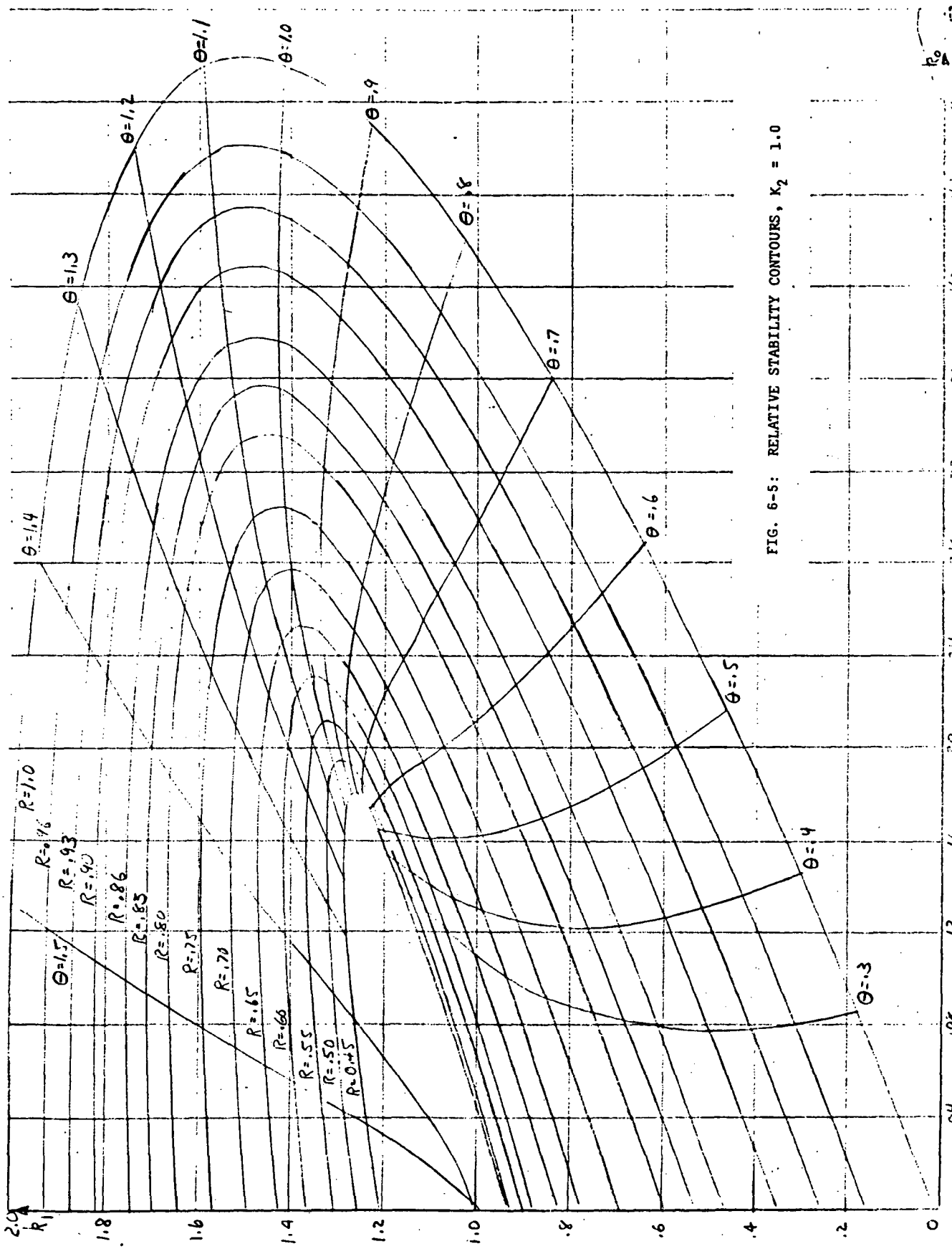

FIG. 6-5: RELATIVE STABILITY CONTOURS, $K_2 = 1.0$

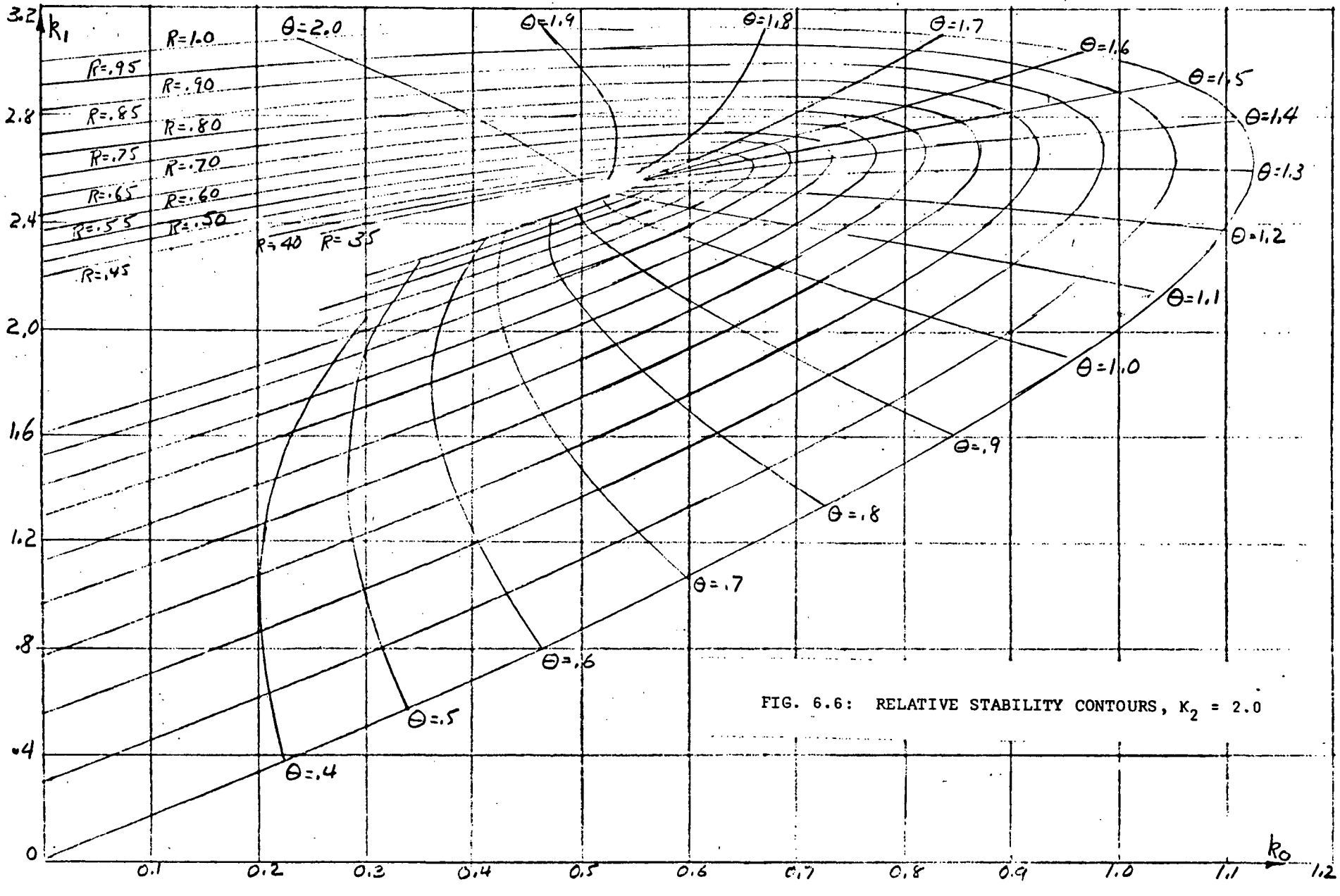

FIG. 6.6: RELATIVE STABILITY CONTOURS, K_2 = 2.0

Since $R = e^{-\zeta W_n T}$ and $\theta = W_n T(1 - \zeta^2)^{1/2}$

i.e., $\log_e R = -\zeta W_n T$ and $\frac{\log_e R}{\theta}(1 - \zeta^2)^{1/2} = -\zeta$

set $\frac{\log_e R}{\theta} = A$, we get $\zeta = A(1 + A^2)^{-1/2}$ $W_n T = \theta(1+A^2)^{1/2}$

Figure 6-7 is the computer generated data conversion chart to translate between the R, θ, and ζ, $W_n T$ variables for design purpose.

For example, choose $K_2 = 1$, $R = 0.93$, $\theta = 1.2$ in Fig. D, we find $k_0 = 0.4$, $k_1 = 1.7$, and in Fig. F we find $\zeta = 0.07$ and $W_n T = 1.2$. To check this in Fig. 6 of Seltzer's paper for $k_0 = 0.4$, $k_1 = 1.7$, one finds $\zeta = 0.07$ and $W_n T = 1.2$. To choose a point within the unit circle of the Z-plane and measure R and θ ($0 \leq \theta < 2\pi$) we can immediately define its corresponding ζ and $W_n T$ values for a certain third parameter K_2. The process can be reversed, i.e., for a given ζ and $W_n T$, we can, through using Fig. 6-7, find the corresponding R and θ. The purpose of using R - θ variables instead of ζ - $W_n T$ is for the convenience of choosing a point in the Z-plane. Once $W_n T$ is found, for a predicted system natural frequency W_n, one can find the sampling time T.

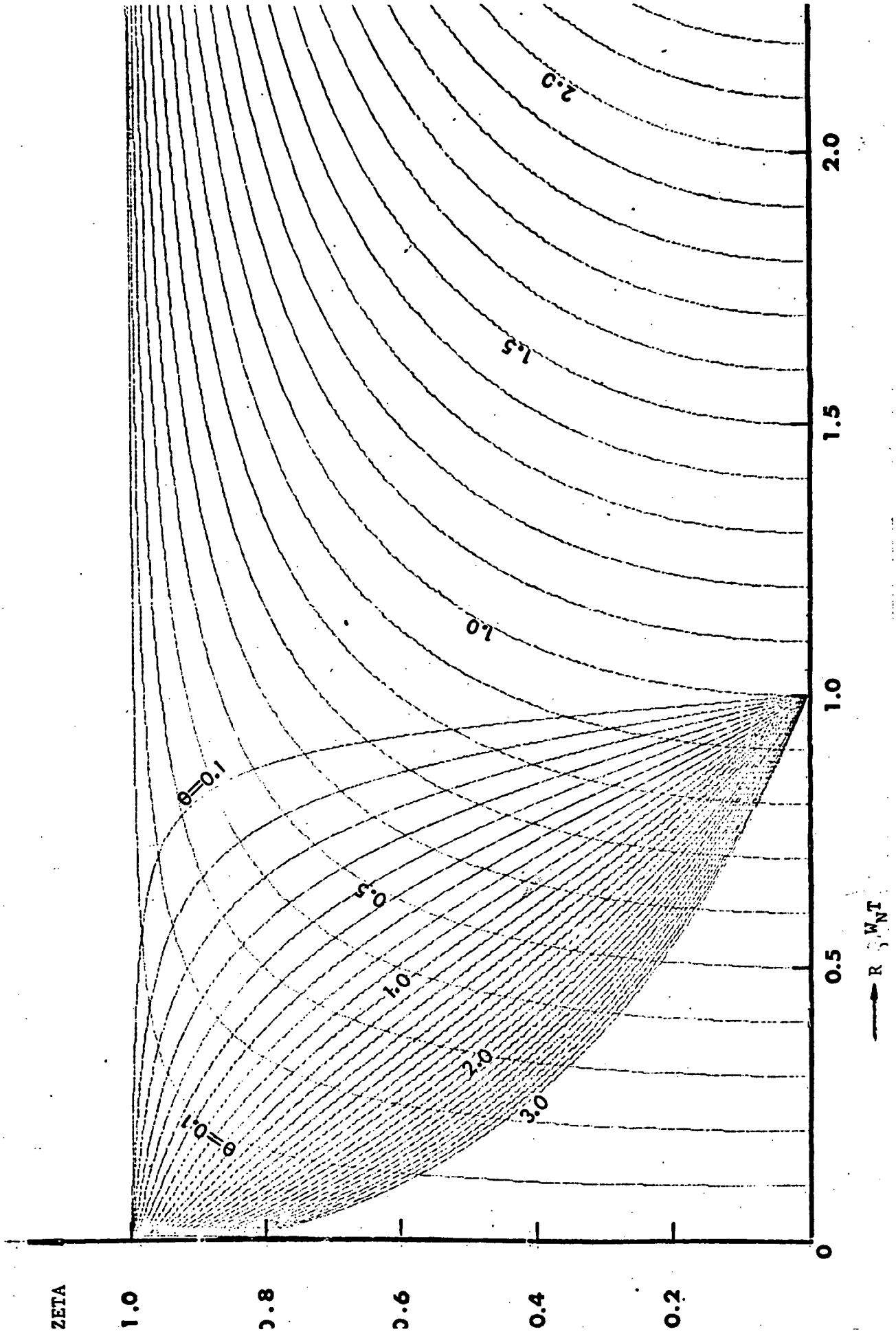

FIG. 6.7: DATA CONVERSION CHART BETWEEN (R-Θ) AND (ζ-$W_N T$) CURVES

b. Simulation Results

One purpose of this project was to explore the possibility of applying stability theory to the definition of regions in the state space which the terminal state is guaranteed to reach from some defined set of initial conditions. Digital simulation was undertaken to provide "experimental" data which could be used to verify the conclusions drawn from the theoretical studies. This section describes the simulation program and some of the pertinent results.

The block diagram used to represent the system in the simulation studies is given in Fig. 6.7a. This was modeled in the IBM 360 computer using the CSMP-360 program. The original program is given in Fig.6-8, with a set of parameter numbers and initial conditions. Note that the two blocks, BETA and GAMMA, shown in Fig. 6-7a,were inserted for gain adjustment and distribution studies. It was thought that the location of gain with respect to the non-linear element might alter performance, but this was found to be untrue as far as stability is concerned.

The numerical values selected, K0 = .292, K1 = 1.146, T = 1. and DEL3 = .1 were used rather than those supplied for the Skylab because simple numbers were desired for the initial theoretical studies (which would include some long-hand calculations). Note that trapezoidal integration was used to avoid problems at the discontinuities, and the integration interval was DELT = .01, which turned out to be too large an interval. Fig. 6-9 a, b, c, show phase plane plots of system response to initial conditions. The

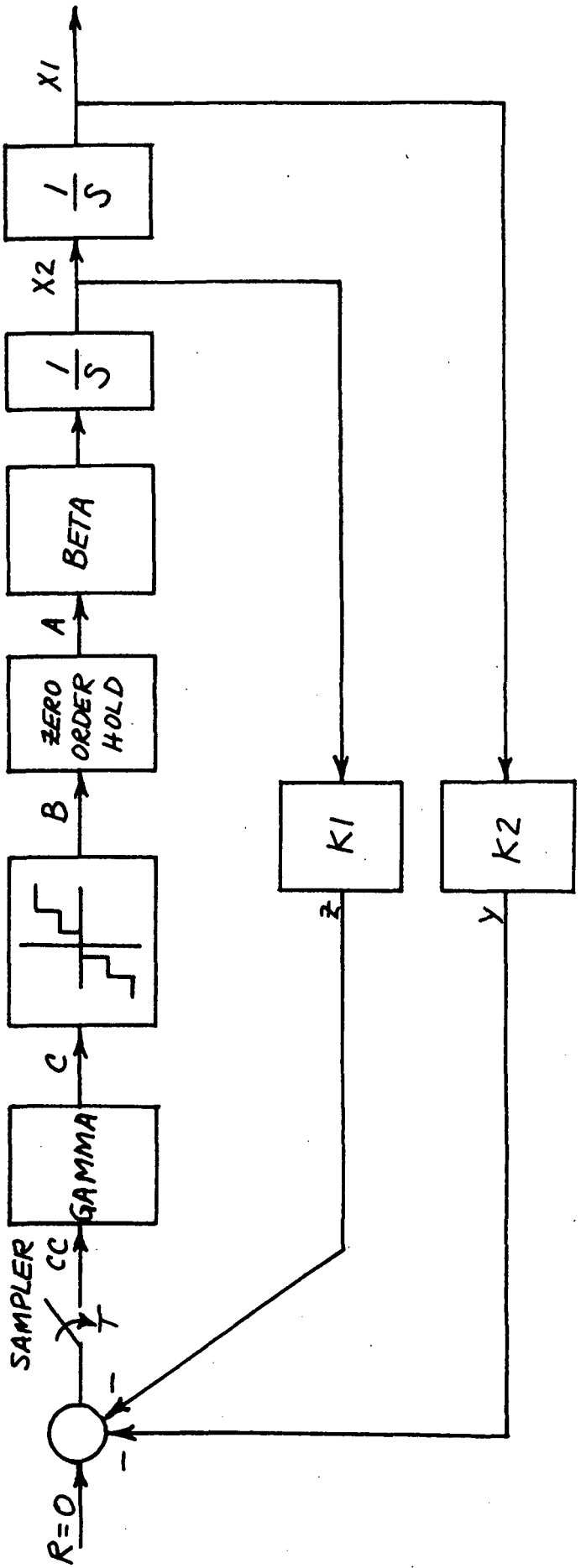

FIG.6-7a: BLOCK DIAGRAM OF SYSTEM USED FOR SIMULATION

```
****CONTINUOUS SYSTEM MODELING PROGRAM****

***PROBLEM INPUT STATEMENTS***

LABEL   STABILITY CMG
PARAMETER K0=.292
PARAMETER K1=1.146
PARAMETER  BETA=1.
PARAMETER GAMMA=1.
PARAMETER   T=1.
PARAMETER  DEL3=.1
PARAMETER   P1=0.

INCON   XA=1.,XB=2.
HISTRY  ZHOLD(100)

        X1=INTGRL(XA,X2)
        X2=INTGRL(XB,BETA*A)
        A=ZHOLD(S,B)
        B=CNTZR(DEL3,C)
         C=GAMMA*CC
         CC=ALPHA*D
        S=ALPHA
        ALPHA=IMPULS(P1,T)
        D=-Y-Z
        Z=K1*X2
        Y=K0*X1
METHOD  TRAPZ
PREPAR  X1,X2
PRINT   X1,X2,A
TIMER FINTIM=500.,DELT=.01,PRDEL=1.
END
STOP
```

FIG. 6-8: INITIAL PROGRAM

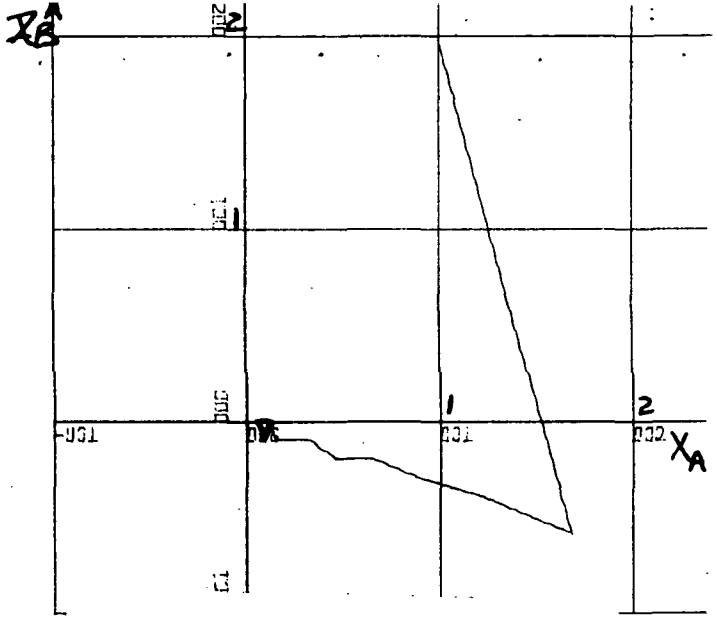

FIG. 6-9a: BETA = 1.0,

GAMMA = 1.0, XA = 1.0, XB = 2.0

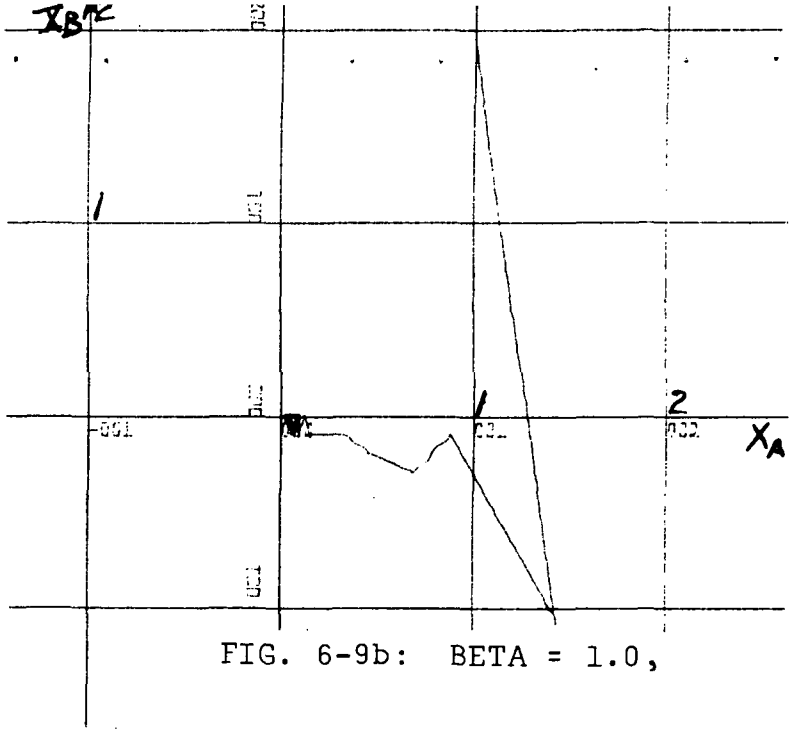

FIG. 6-9b: BETA = 1.0,

GAMMA = 1.2, XA = 1.0, XB = 2.0

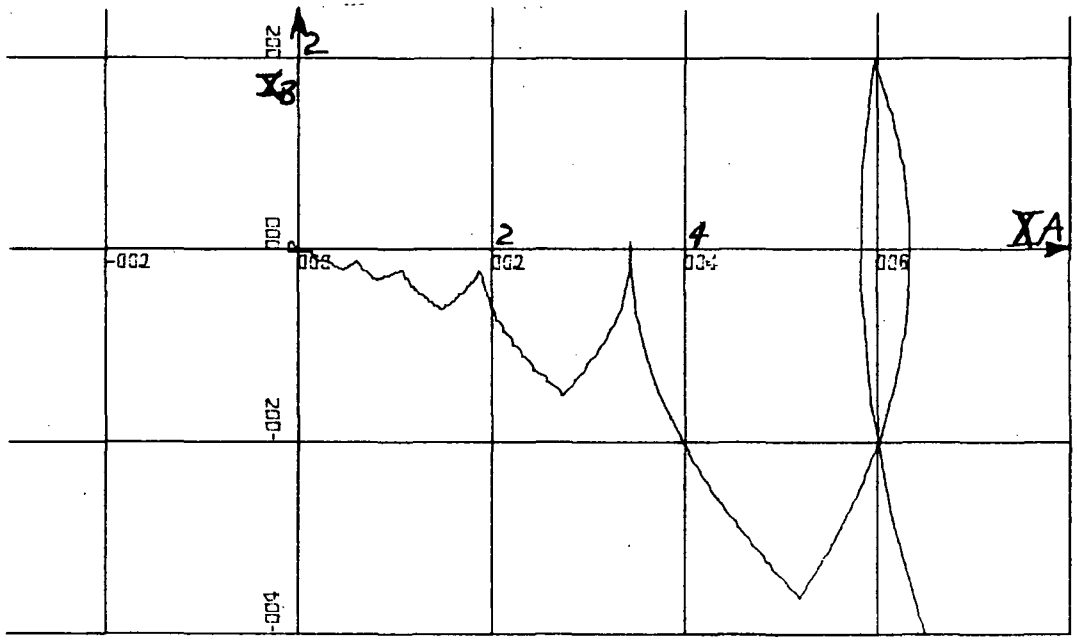

FIG. 6-9c: BETA = 1.0, GAMMA = 1.4, XA = 10.0, XB = - 10.0

terminal portion of the trajectories shows what appears to be a limit cycle. The plots, however, are rather crude because the time increment was too large and the scale plots poorly chosen. It was decided to get plots with better portrayal of the cycles, so the program was rerun with better plot scales and with smaller time increment and smaller integration interval. Typical results are shown in Fig. 6-10. Note that the supposed limit cycles have disappeared. The obvious cause of the discrepancy is the integration interval. This is mentioned in the report because the proposed Skylab will use an on-line time shared digital computer, and the position and velocity measurements are quantized for use in this computer. Thus, if the integration interval or measurement granularity are chosen too large, a situation such as we have observed may be encountered.

To continue the simulation studies the loop gain was varied to find a value for which the system would exhibit oscillatory characteristics. This was done to inverse the probability of finding limit cycles, since a part of the theoretical study is concerned with such phenomena. It was found that for relatively modest gain increases the system damping changes substantially.

For K0 = .292, K1 = 1.146, BETA = GAMMA = 1, the system is heavily damped, exhibiting characteristics similar to the chatter mod- of relay servos. Changing only GAMMA, it was found that at GAMMA = 1.8 the system appears to be divergingly unstable. It was decided that GAMMA = 1.6 was a suitable value for our purposes.

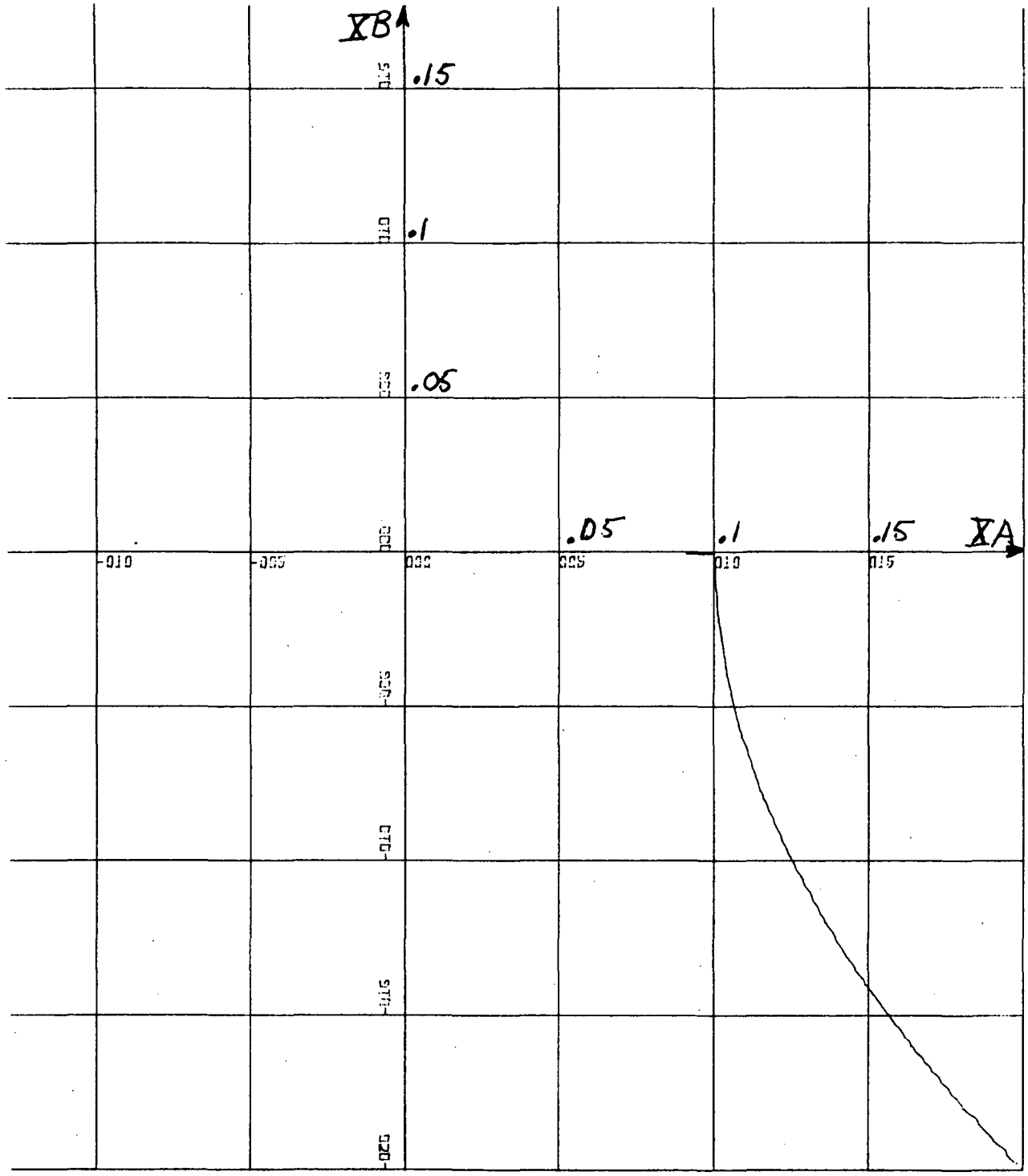

FIG. 6-10a: BETA = 1.0, GAMMA = 1.4, XA = 0.2, XB = - 0.2

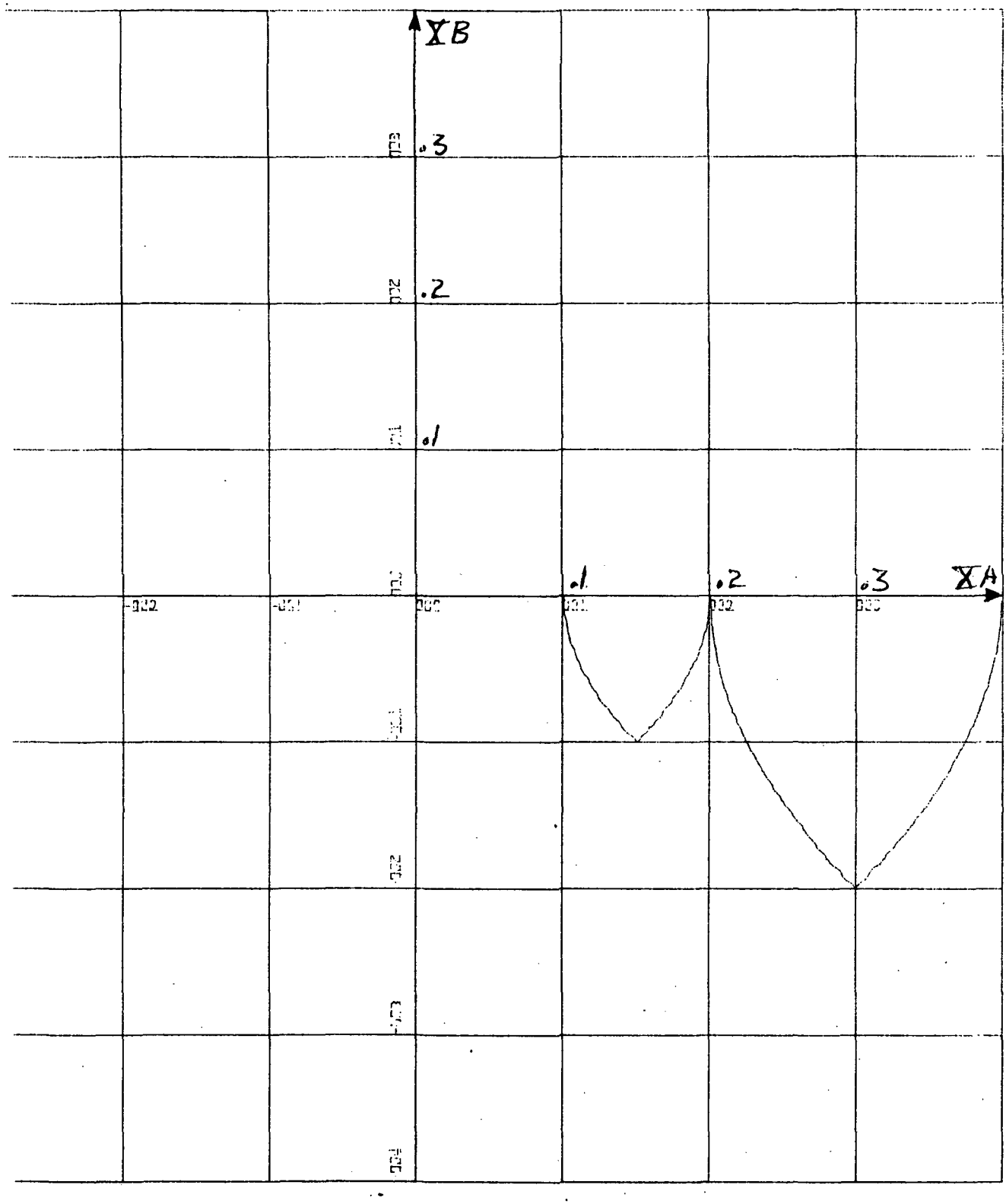

FIG. 6-10b: BETA = 1.0, GAMMA = 1.4, XA = 0.4, XB = 0.0

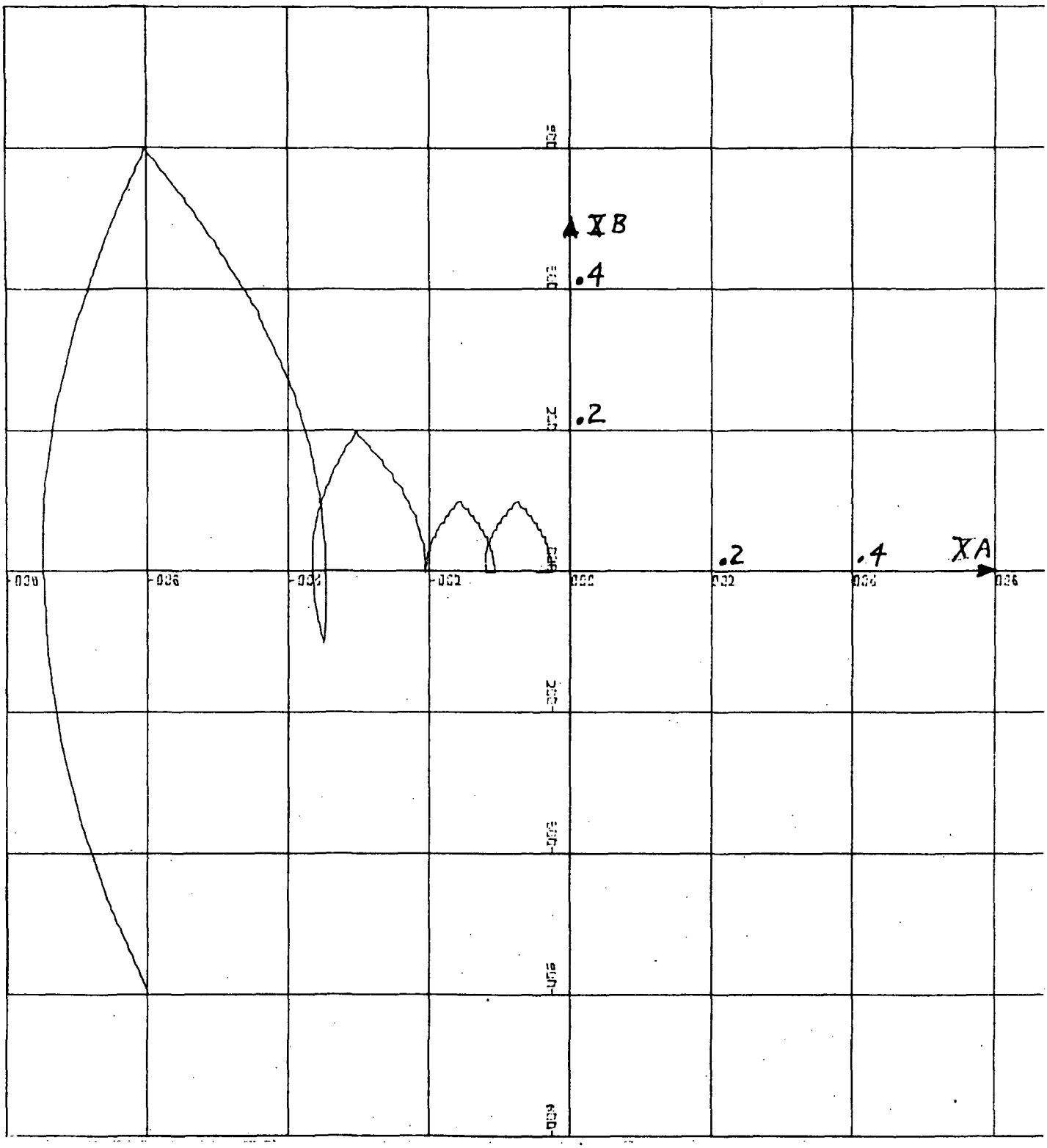

FIG. 6-10c: BETA = 1.0, GAMMA = 1.4, XA = XB = - 0.6

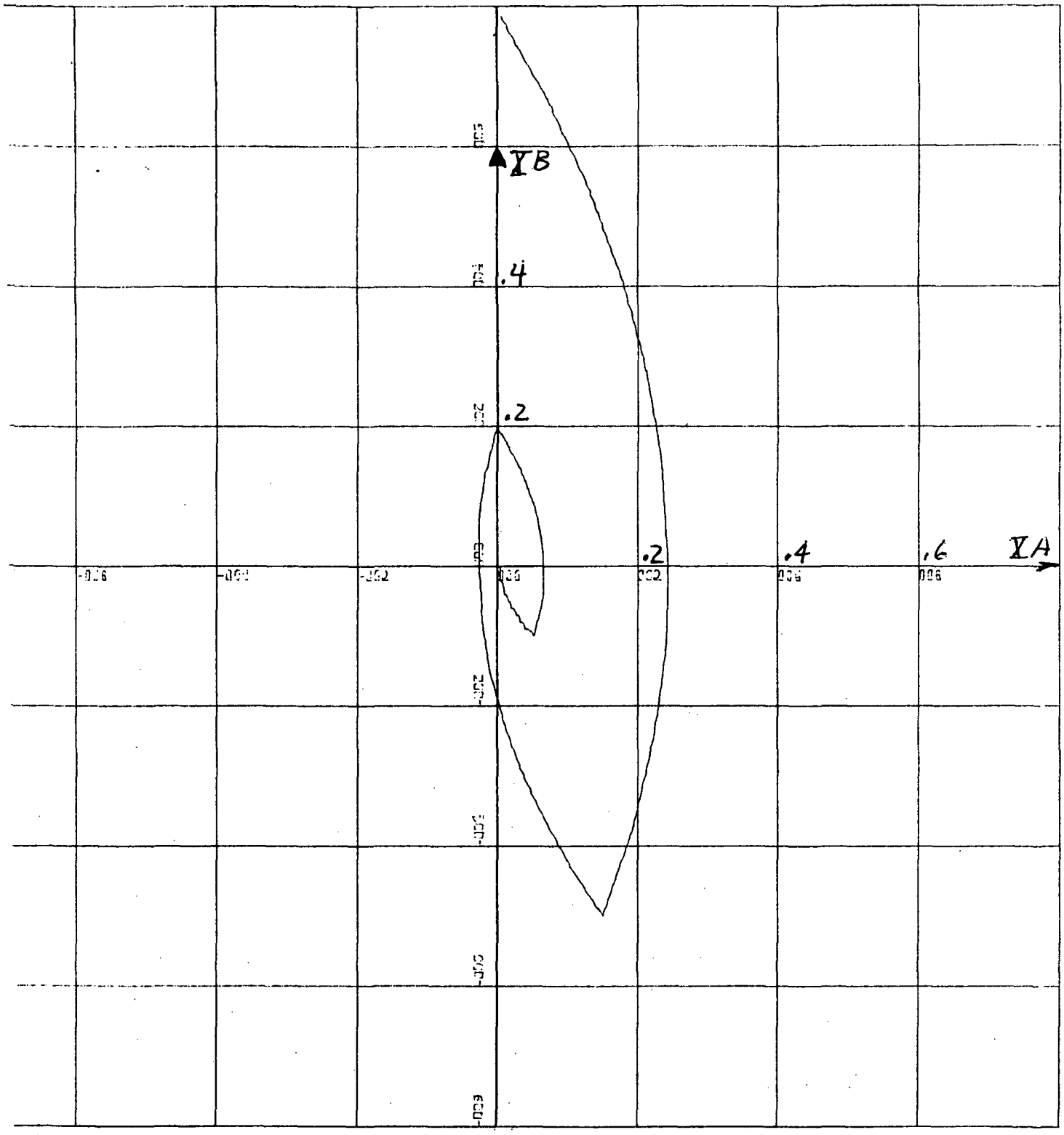

FIG. 6-10d: BETA = 1.0, GAMMA = 1.4, XA = 0.0, XB = 0.8

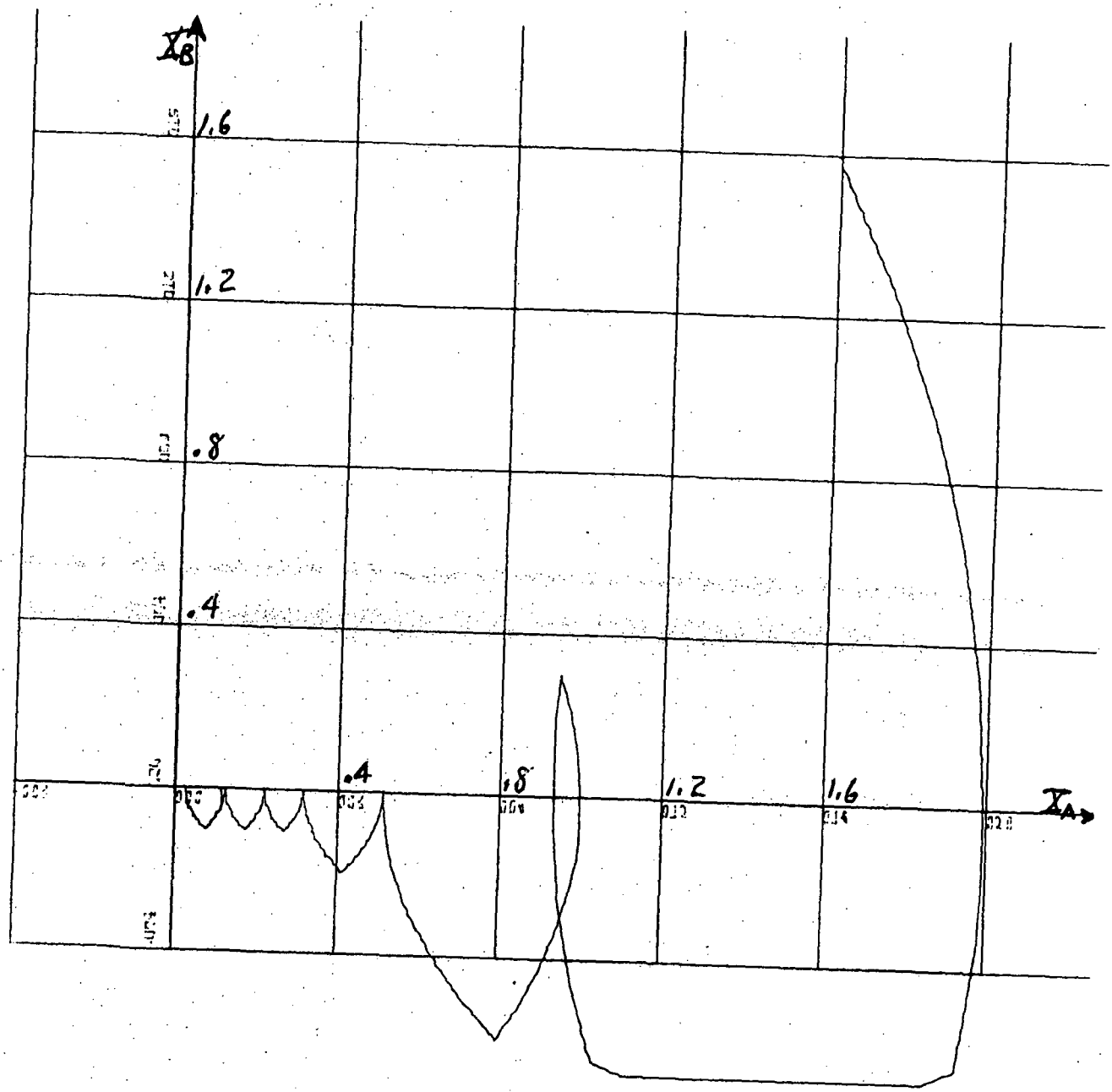

FIG. 6-10e: BETA = 1.0, GAMMA = 1.4, XA = XB = 1.6

All remaining simulation runs were made with the forward gain set at GAMMA = 1.6, and the initial conditions were chosen on a square grid surrounding the origin of the phase plane. A copy of the program is given in Fig. 6.11; it differs from that in Fig. 6-8 only in the value of GAMMA, the integration interval, and the run time, print interval, etc. The results for this increased gain condition not only differ amazingly from those in Fig. 6-10,but showed some surprising symmetries which can be described briefly. First, the responses showed symmetry in a polar sense, i.e., initial conditions in the first and third quadrants gave responses which were identical in a polar symmetry sense, as were responses to initial conditions in the second and fourth quadrants. Initial conditions of position only gave comparatively well damped responses, with no chatter or limit cycles for small values of initial condition, but exhibited a chatter mode type of limit cycle* as it approached but did not reach the origin. Initial conditions of velocity only went immediately into a limit cycle type of oscillation about the origin, and as the magnitude of this initial condition increased several such modes of different amplitudes appeared. Initial conditions in the first and third quadrants gave limit cycles that did not enclose the origin. while initial conditions in the second and fourth quadrants gave limit cycles that did enclose the origin.

Because of the symmetries noted above, the results presented do not contain all of the data obtained but just representative

*Note tne term limit cycle is used rather loosely here to describe a type of motion which is not precisely a limit cycle. This is discussed later.

```
                ****CONTINUOUS SYSTEM MODELING PROGRAM****
      ***PROBLEM INPUT STATEMENTS***

LABEL   STABILITY CMG
PARAMETER KO=.292
PARAMETER K1=1.146
PARAMETER  BETA=1.,GAMMA=1.6
PARAMETER  T=1.
PARAMETER  DEL3=.1
PARAMETER  P1=0.

INCON  XA=0.,XB=-1.6
HISTRY  ZHOLD(100)

       X1=INTGRL(XA,X2)
       X2=INTGRL(XB,BETA*A)
       A=ZHOLD(S,B)
       B=CNTZR(DEL3,C)
        C=GAMMA*CC
        CC=ALPHA*D
       S=ALPHA
       ALPHA=IMPULS(P1,T)
       D=-Y-Z
       Z=K1*X2
       Y=KO*X1
METHOD  TRAPZ
PREPAR  X1,X2
PRINT  X1,X2,A
TIMER  FINTIM=89.,DELT=.001,PRDEL=.1
END
STOP
```

FIG. 6-11: REVISED PROGRAM FOR RESULTS OF FIGURES 6-12 THROUGH 6-15

samples. Fig. 6-12 shows four trajectories starting from an initial position with zero initial velocity. Note that for small values of initial position there is no tendency to cycle, but at large values of initial position some cycling is produced, but does not enclose the origin. Fig.6-13 shows three trajectories starting from an initial velocity with zero initial position. For a small magnitude of initial conditions, the system immediately starts cycling about the origin. For a substantially larger initial velocity two modes of cycling occur as the trajectory approaches the origin, but for a still larger initial velocity one of these modes disappears. Fig.6-14 shows four trajectories starting in the first and third quadrants. All seem to terminate in a type of limit cycle which does not enclose the origin. Fig.6-15 shows four trajectories starting in the second and fourth quadrants. In this case all seem to terminate in a type of limit cycle, but for the smaller initial conditions the cycle does not enclose the origin, while for the larger initial conditions it does.

c. Comments on Simulation Results

From the trajectories shown on Fig. 6-12 through Fig. 6-15, it is clear that the oscillations observed are not limit cycles in the usual sense, since the trajectory is not repeated exactly on successive cycles. There appears to be a "drift", i.e., successive cycles tend to be displaced along the position axis, usually tending toward the origin. There was evidence, in some of the print-out data, that the trajectories eventually reached the

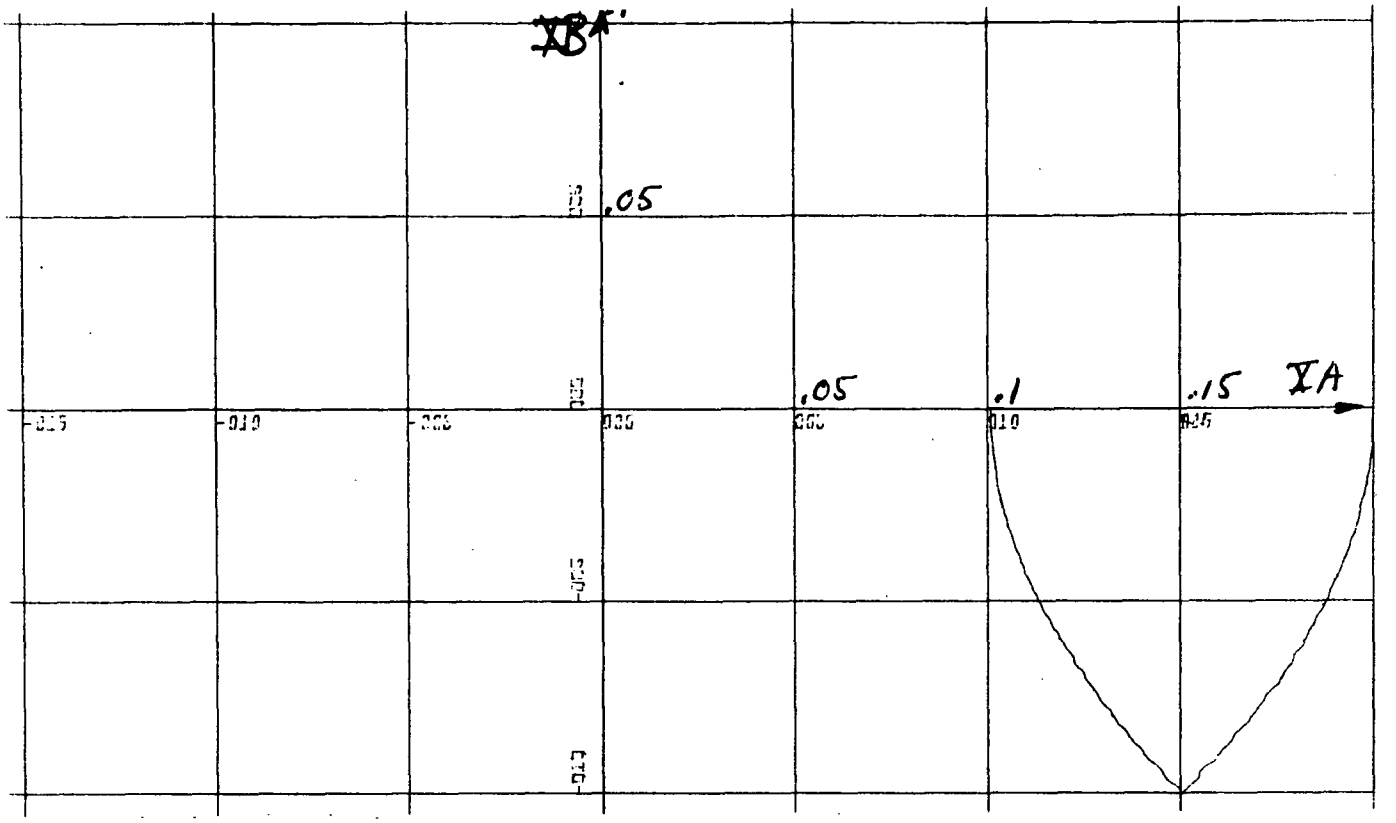

FIG. 6-12a: BETA = 1.0, GAMMA = 1.6, XA = 0.2, XB = 0.0

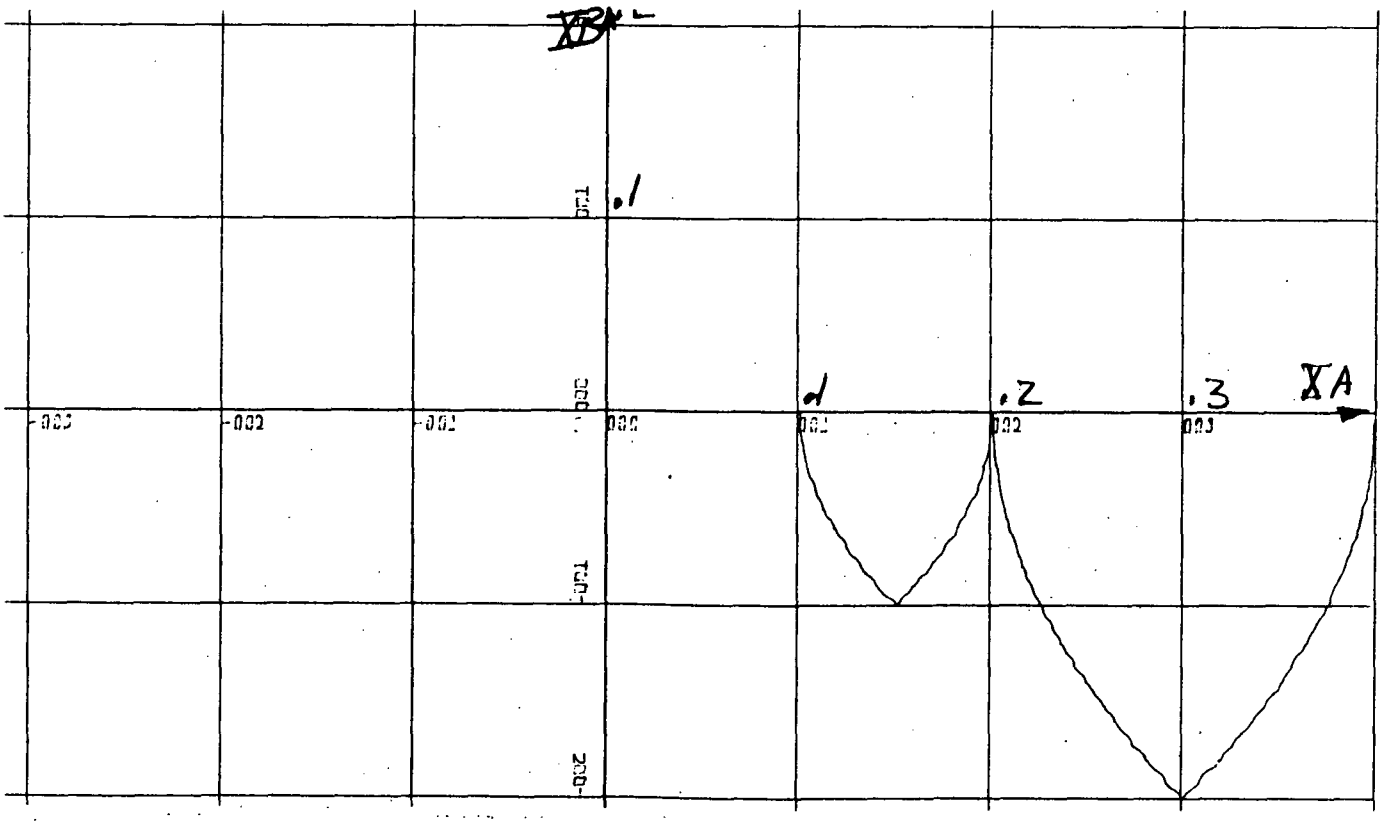

FIG. 6-12b: BETA = 1.0, GAMMA = 1.6, XA = 0.4, XB = 0.0

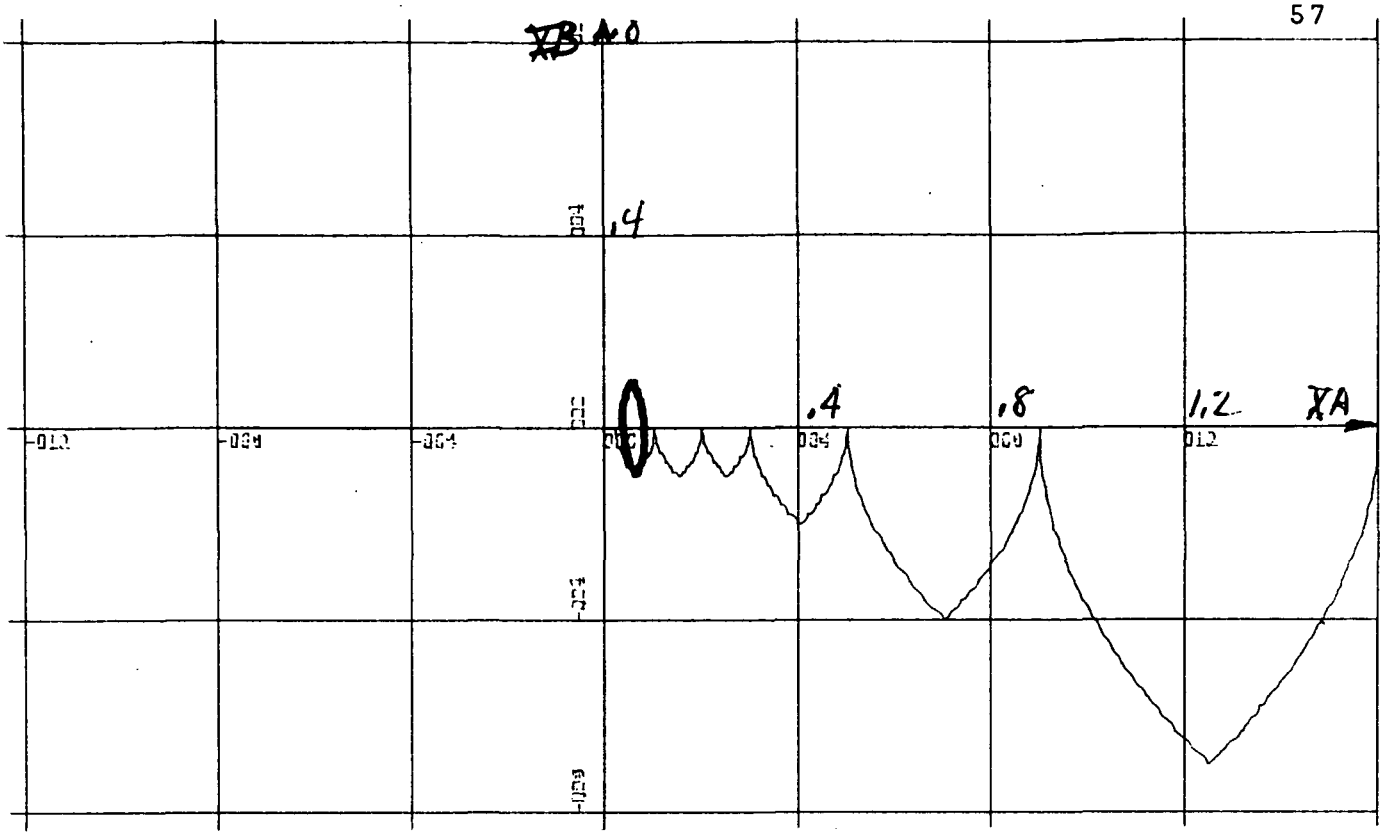

FIG. 6-12c: BETA = 1.0, GAMMA = 1.6, XA = 1.6, XB = 0.0

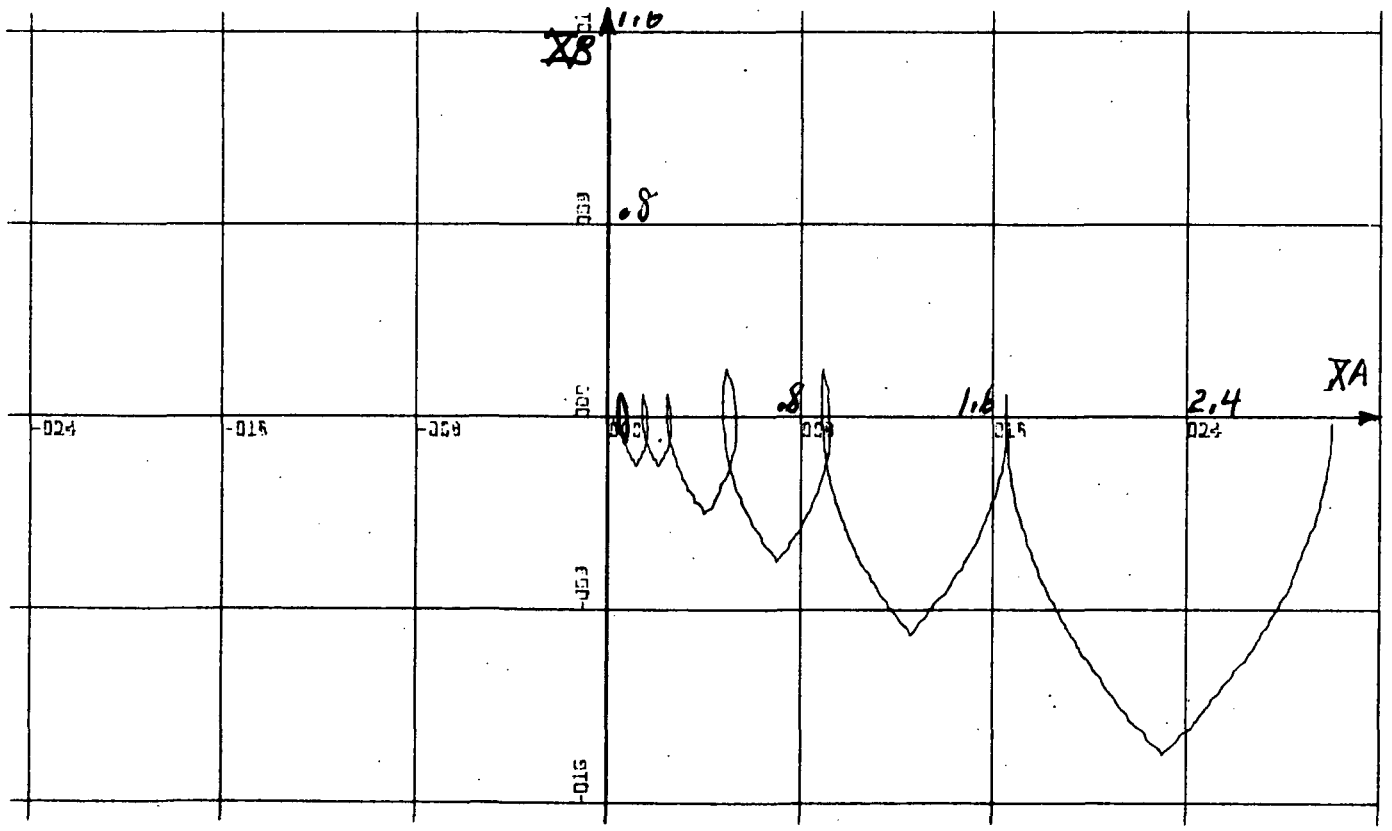

FIG. 6-12d: BETA = 1.0, GAMMA = 1.6, XA = 3.0, XB = 0.0

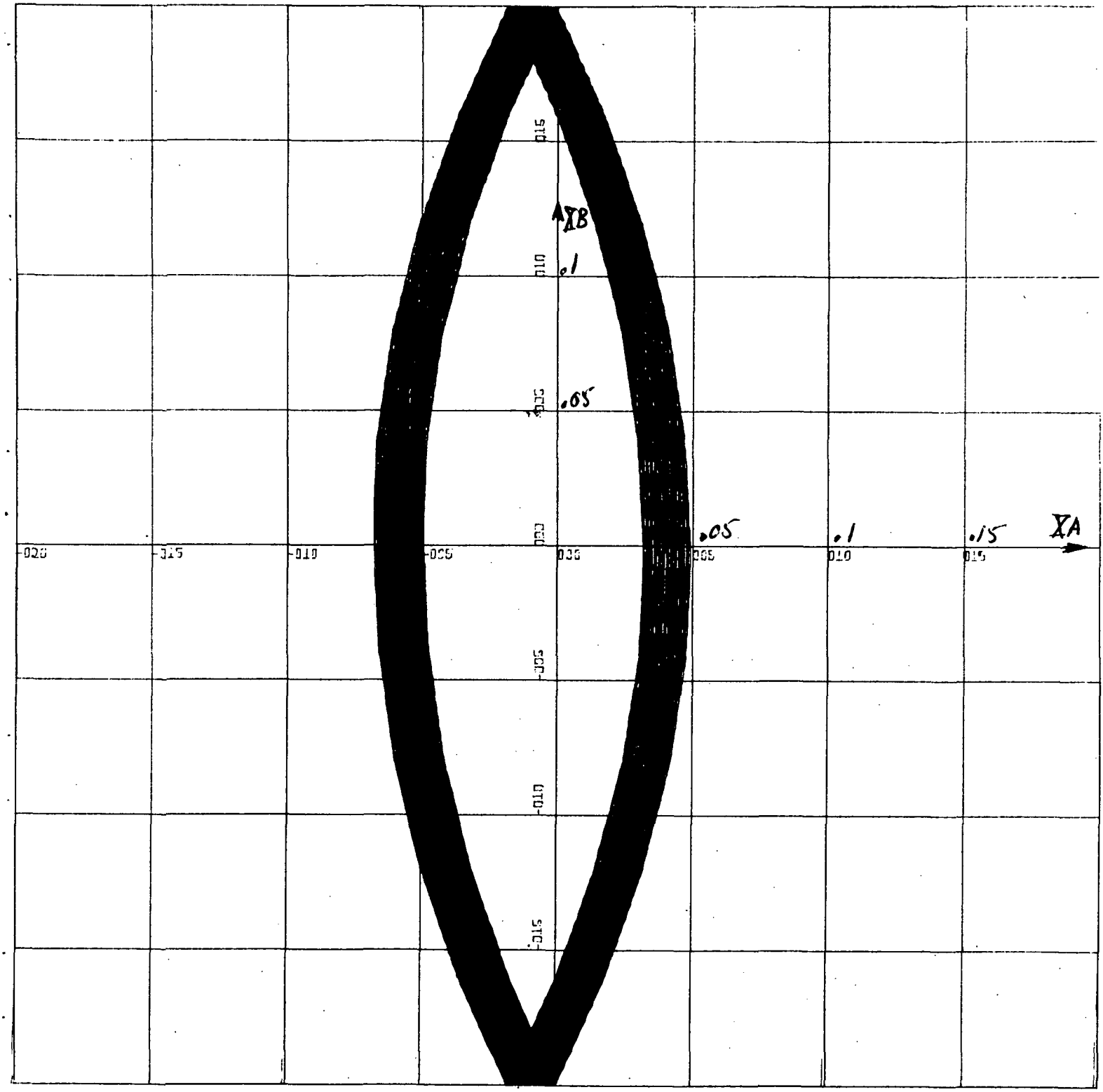

FIG. 6-13a: BETA = 1.0, GAMMA = 1.6, XA = 0.0, XB = - 0.2

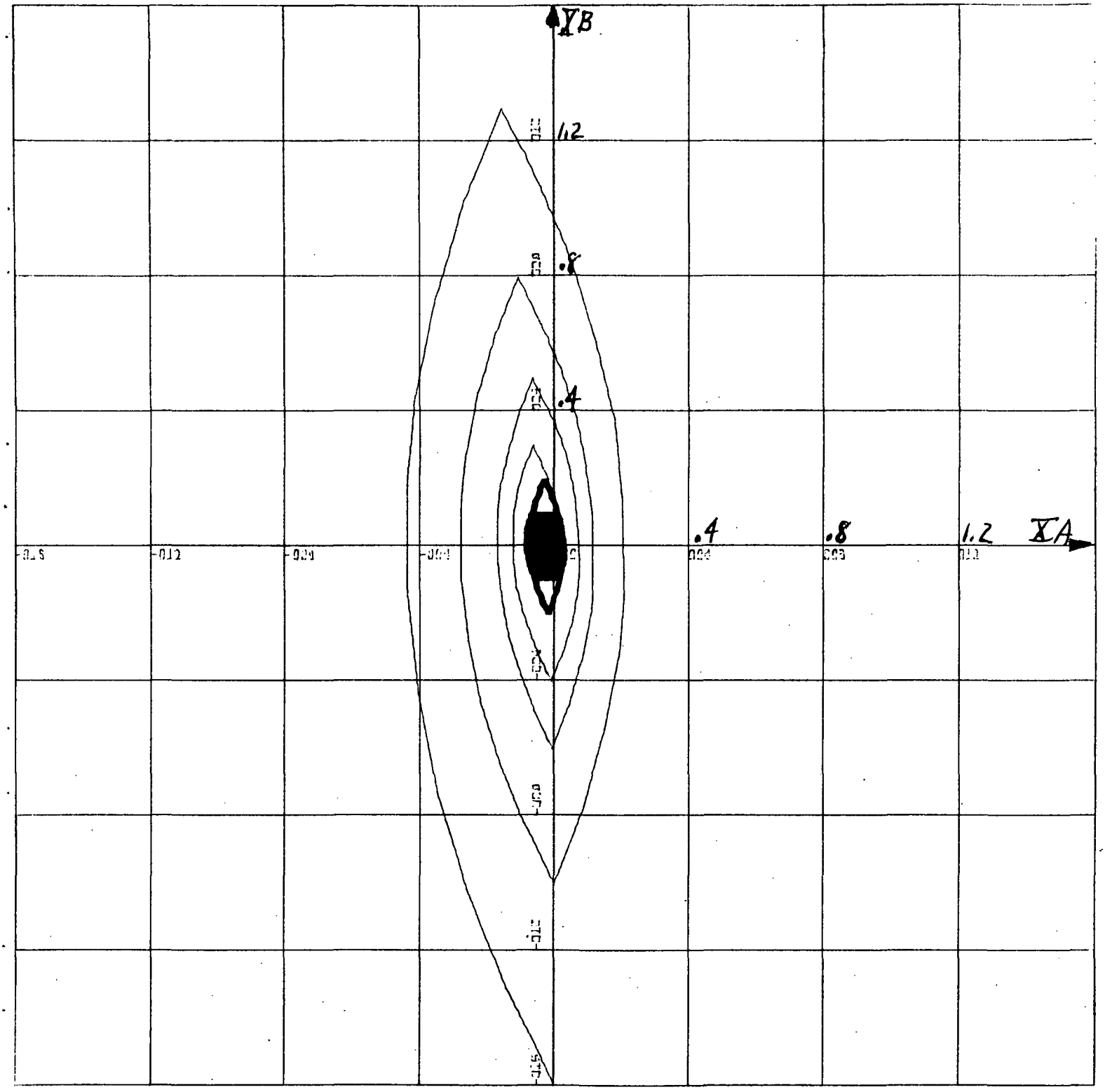

FIG. 6-13b: BETA = 1.0, GAMMA = 1.6, XA = 0.0, XB = 1.6

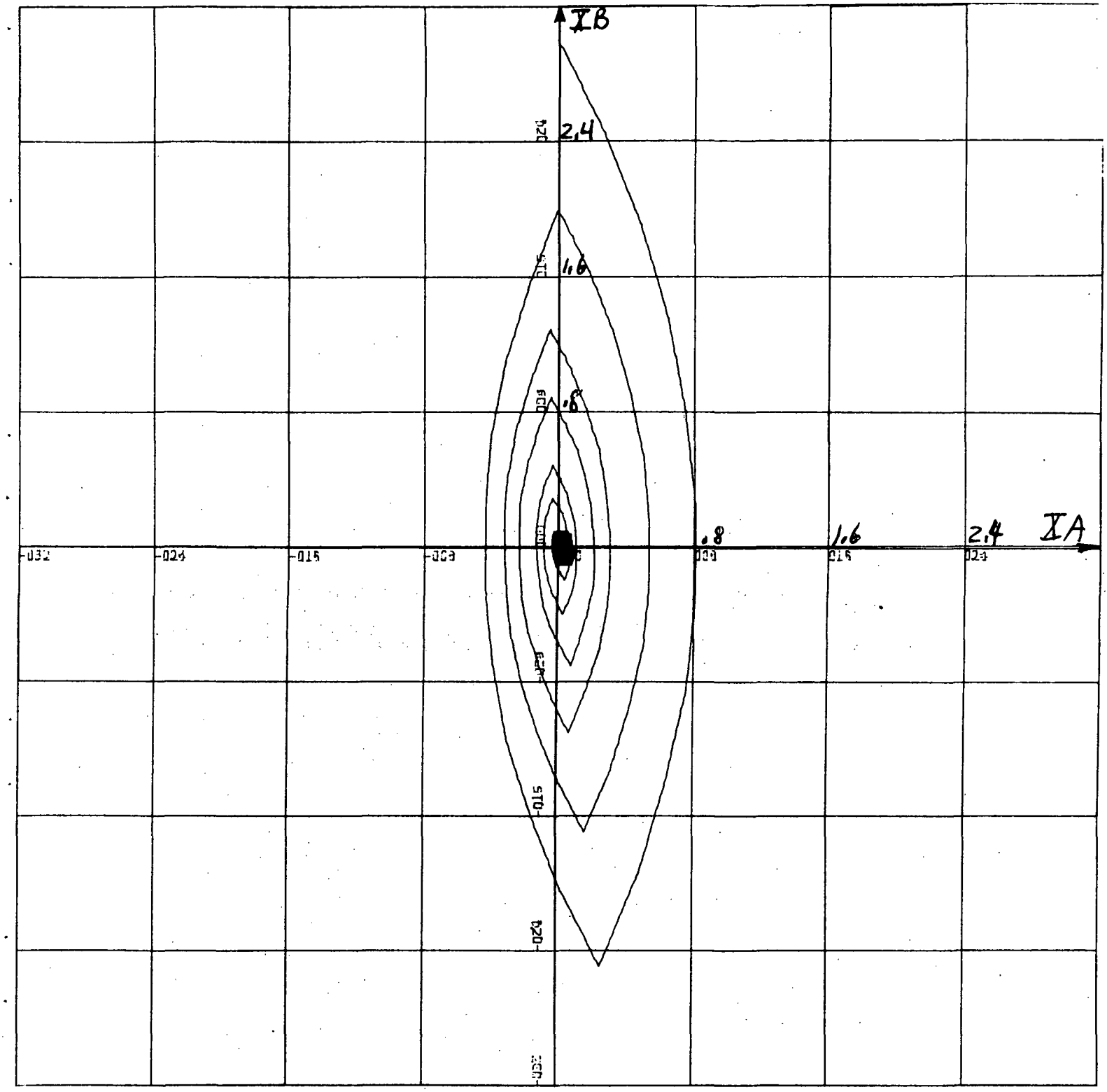

FIG. 6-13c: BETA = 1.0, GAMMA = 1.6, XA = 0.0, XB = 3.0

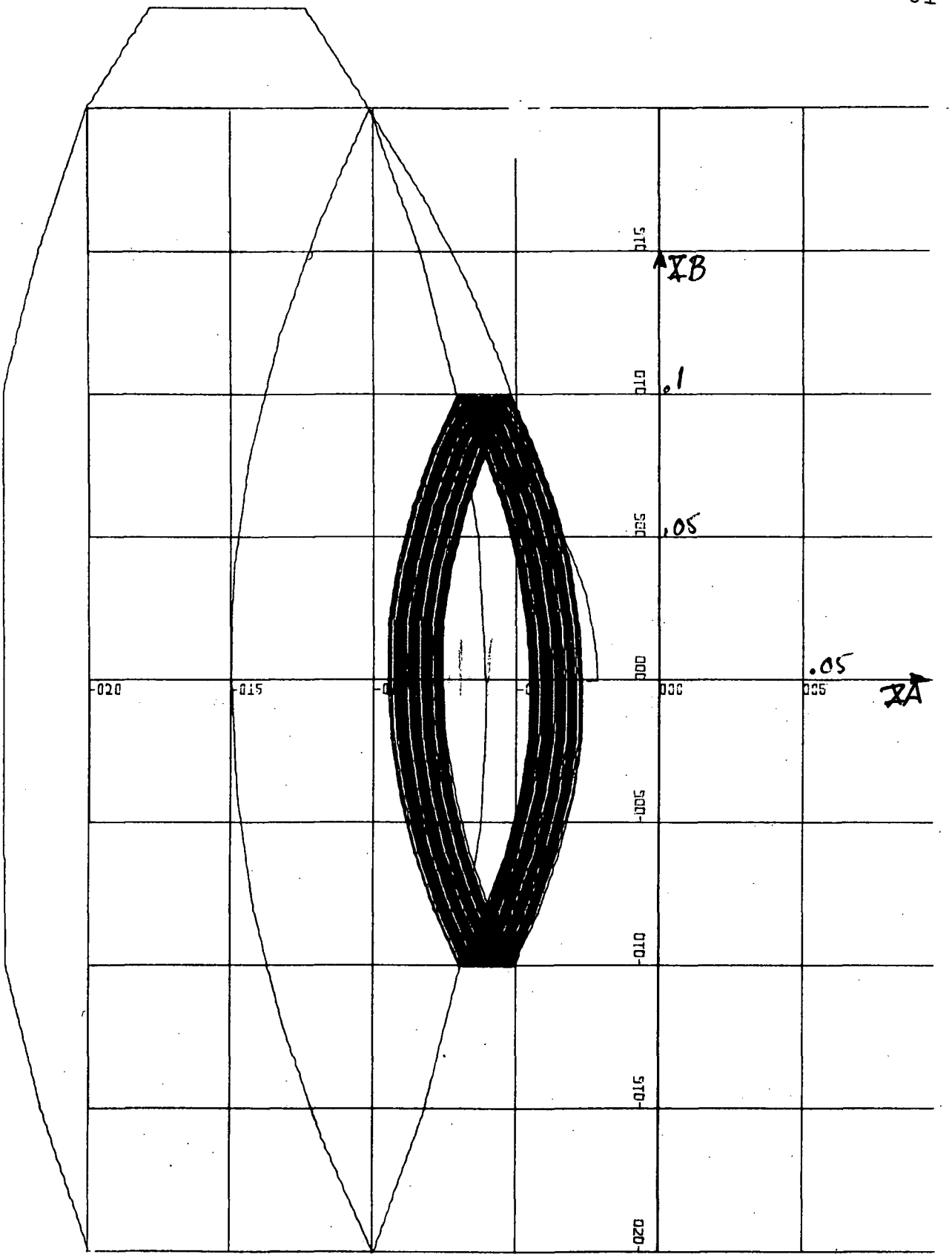

FIG. 6-14a: BETA = 1.0, GAMMA = 1.6, XA = - 0.2, XB = - 0.2

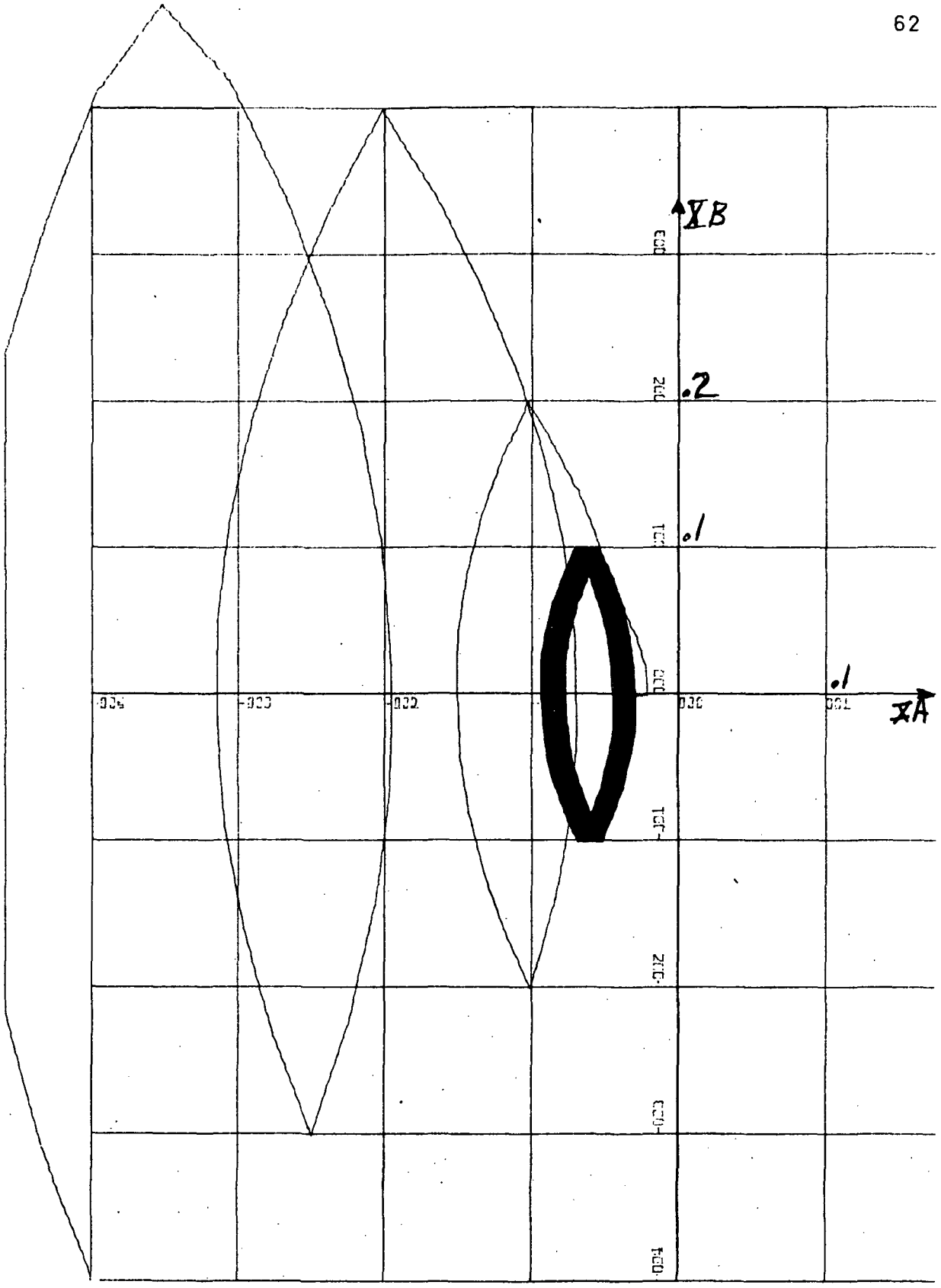

FIG. 6-14b: BETA = 1.0, GAMMA = 1.6, XA = - 0.4, XB = - 0.4

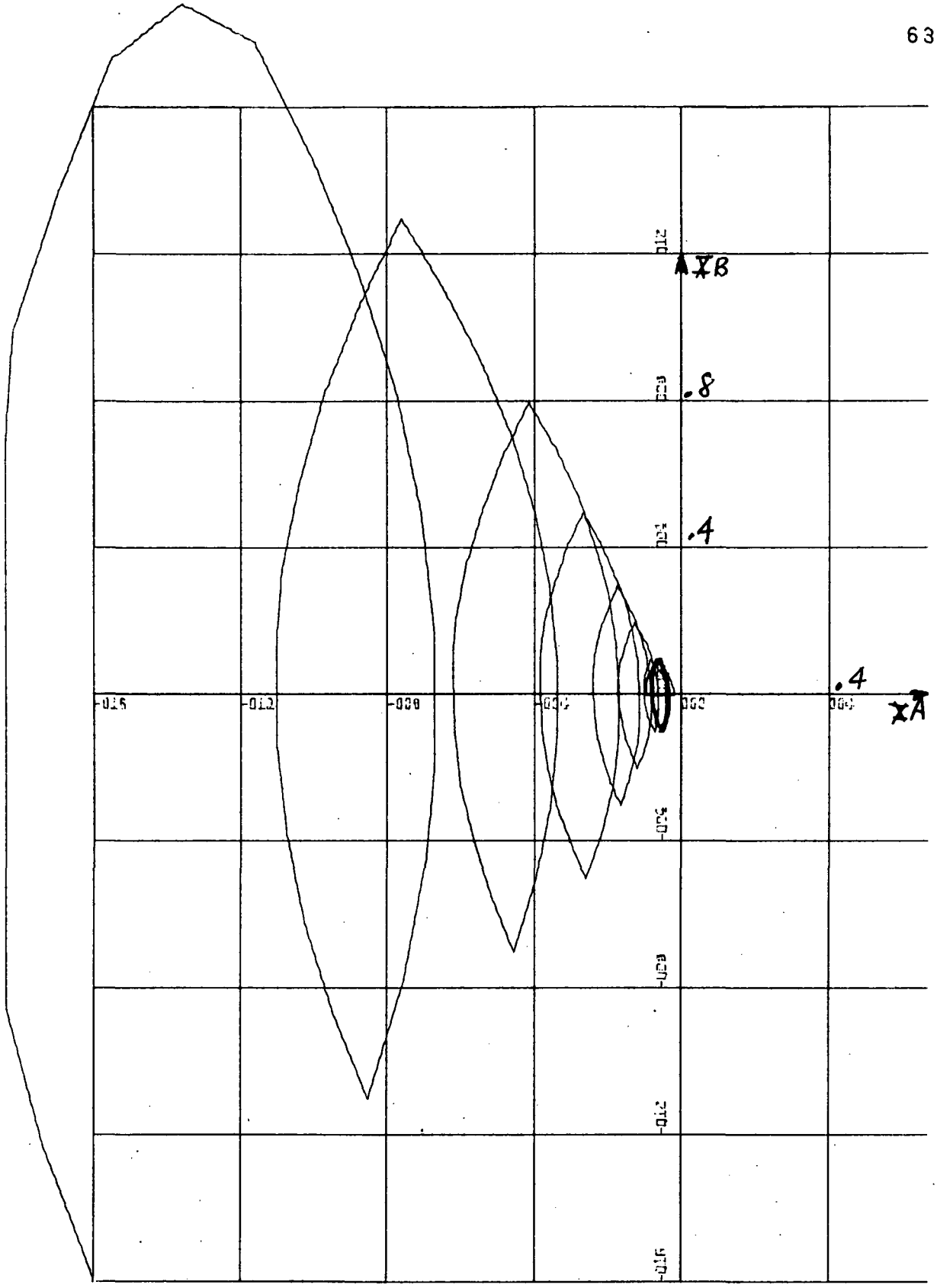

FIG. 6-14c: BETA = 1.0, GAMMA = 1.6, XA = - 1.6, XB = - 1.b

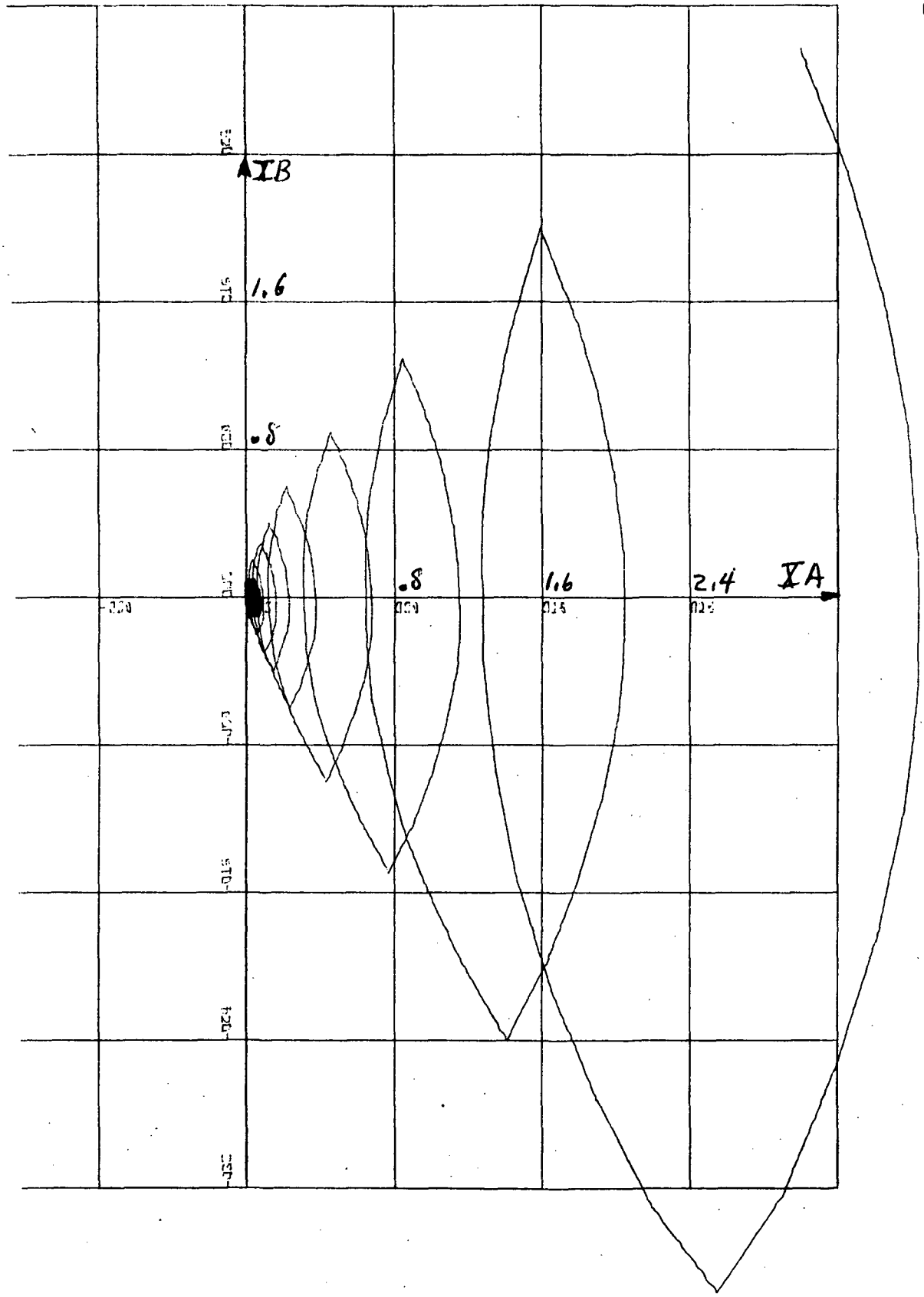

FIG. 6-14d: BETA = 1.0, GAMMA = - 1.6, XA = 3.0, XB = 3.0

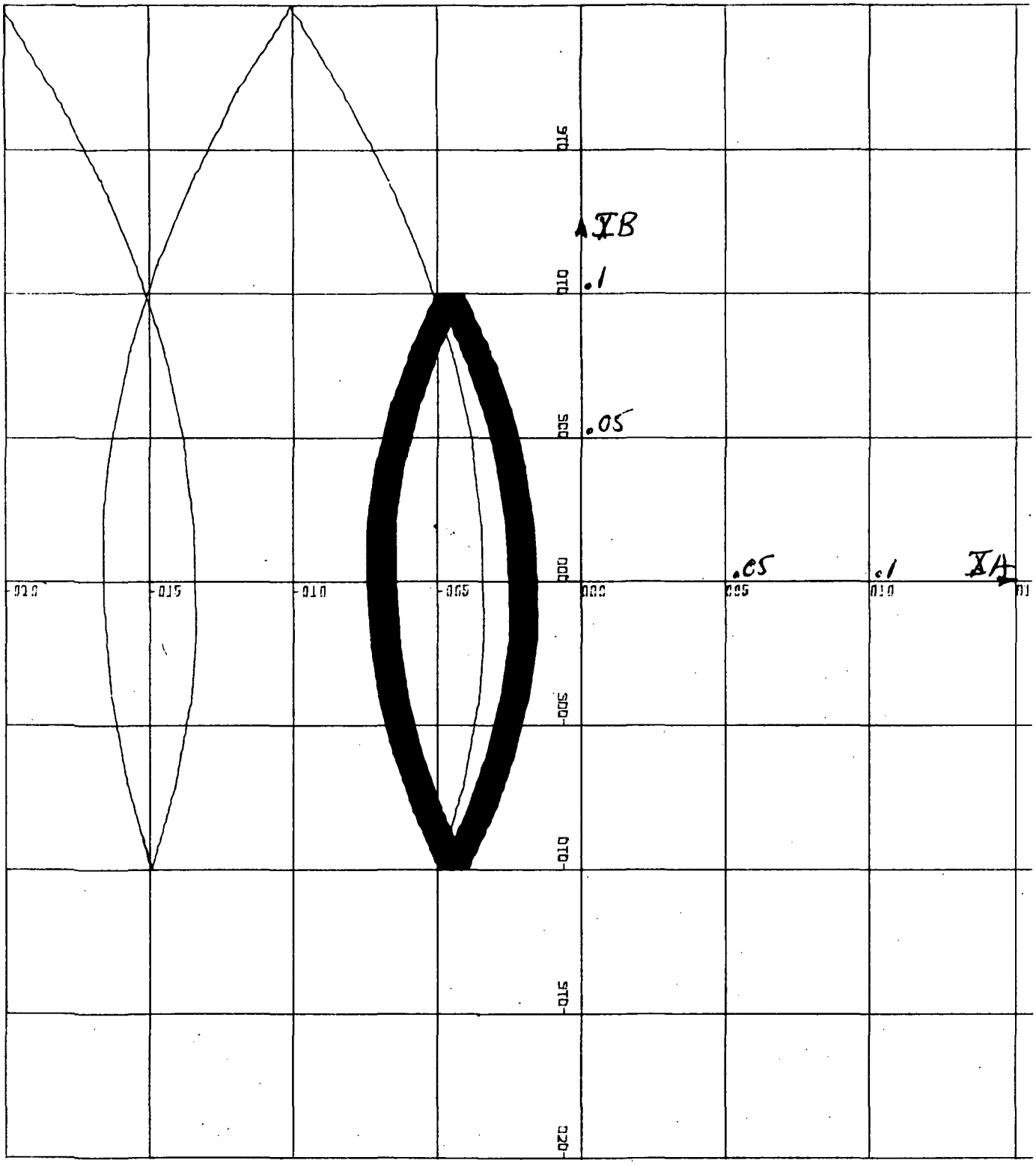

FIG. 6-15a: BETA = 1.0, GAMMA = 1.6, XA = - 0.2, XB = 0.2

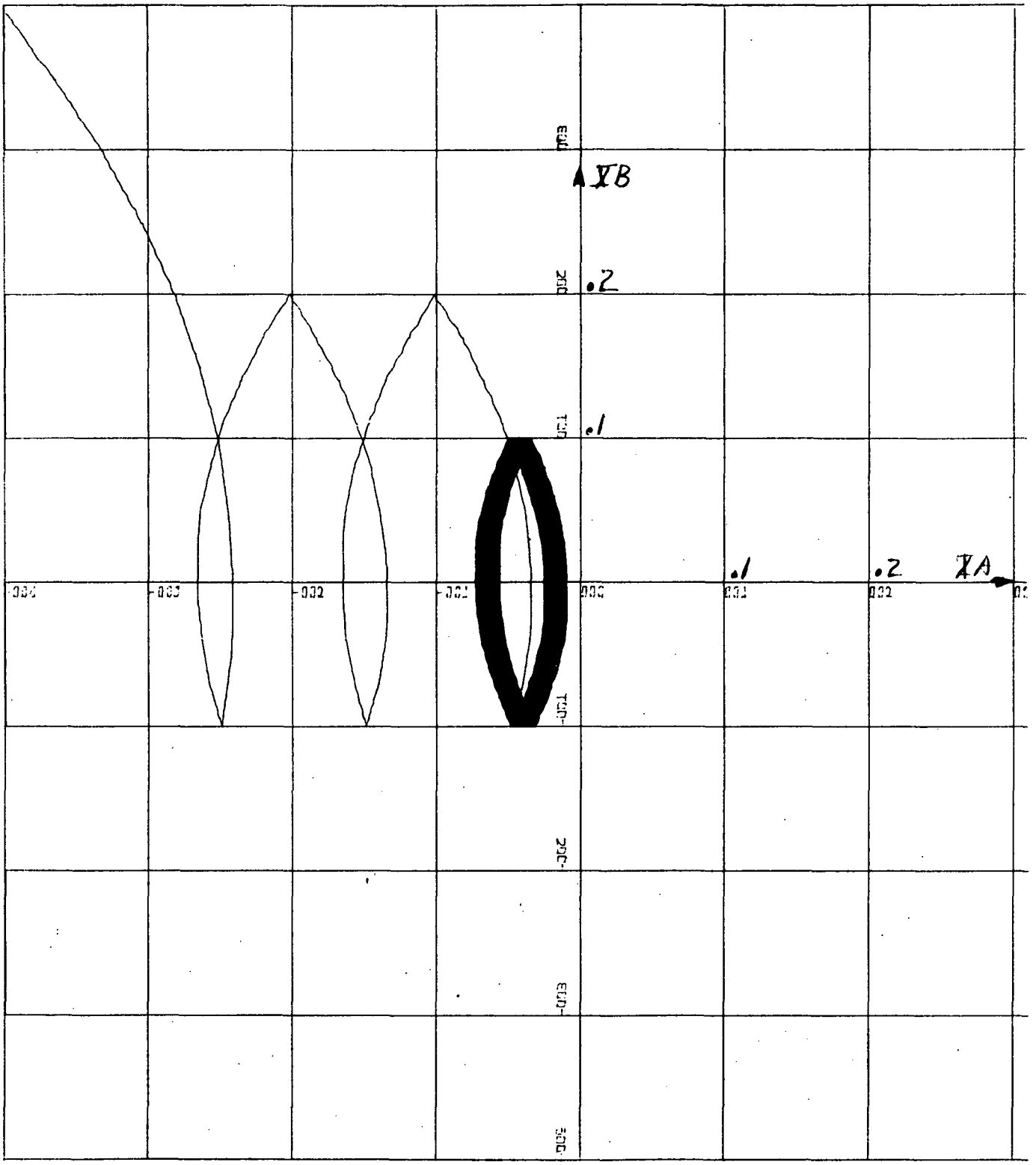

FIG. 6-15b: BETA = 1.0, GAMMA = 1.6, XA = - 0.4, XB = 0.4

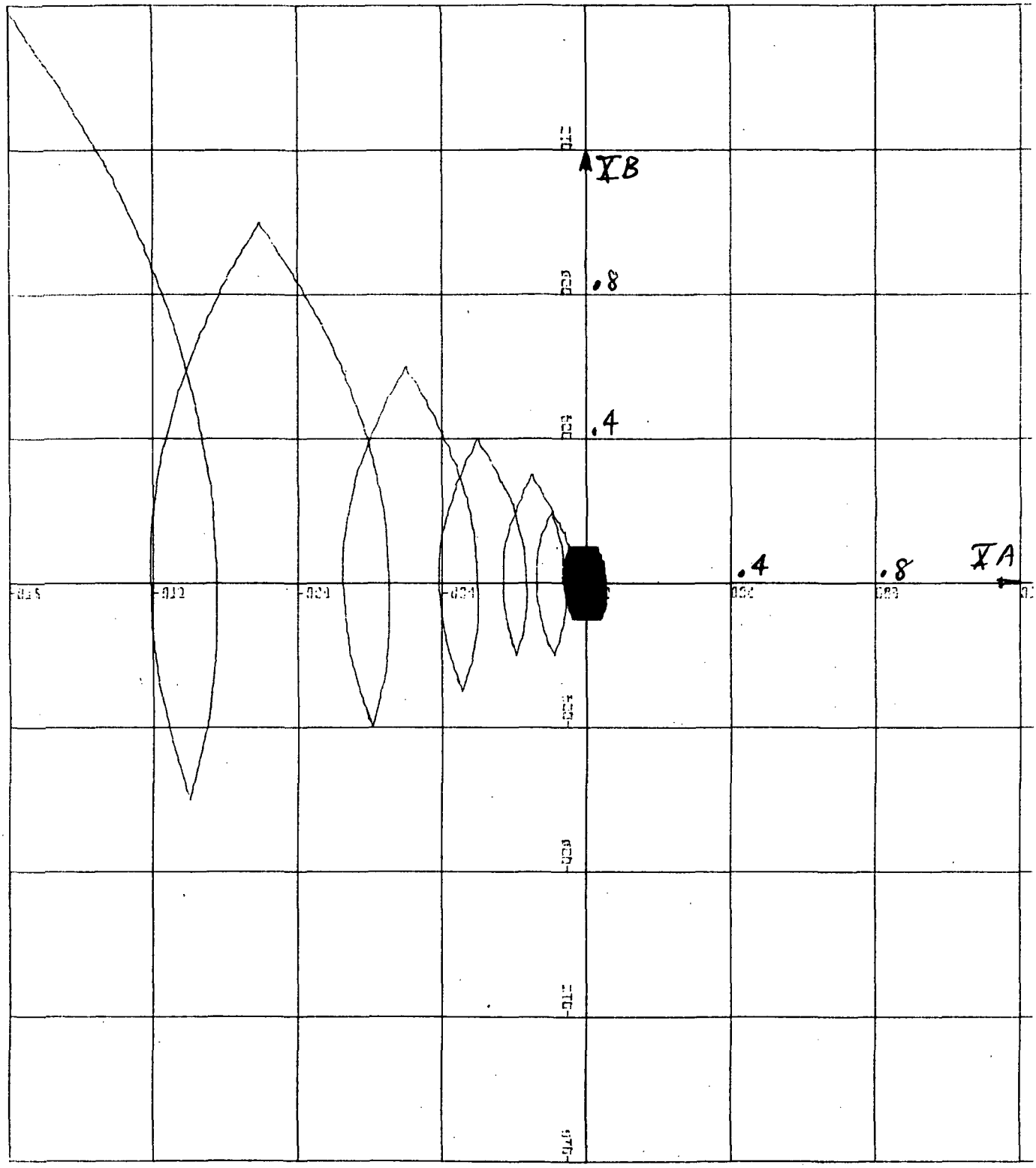

FIG. 6-15c: BETA = 1.0, GAMMA = 1.6, XA = - 1.6, XB = 1.6

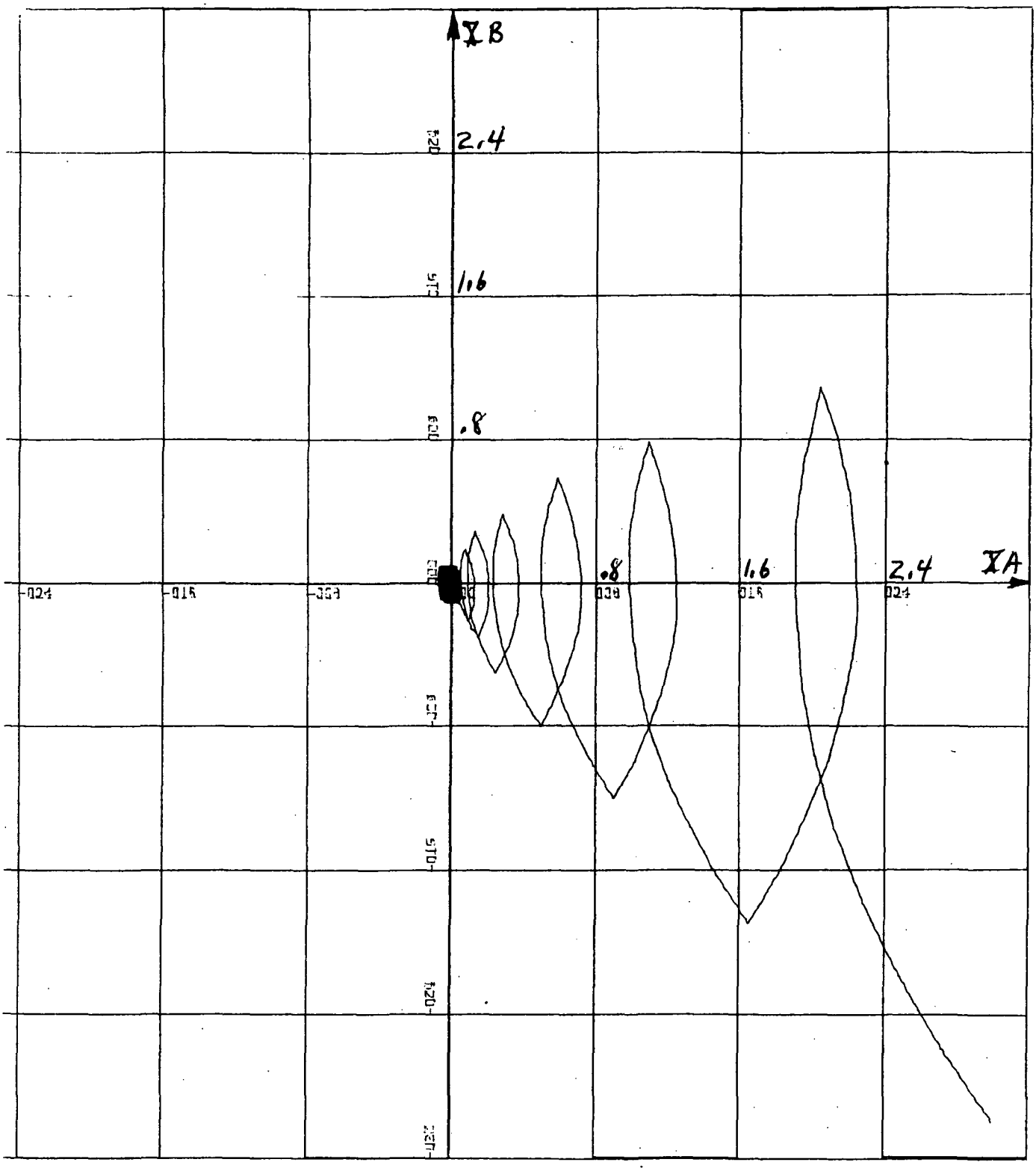

FIG. 6-15d: BETA = 1.0, GAMMA = 1.6, XA = 3.0, XB = - 3.0

dead zone of the quantizer and that a no-power, constant velocity mode followed the cycling mode. Since the model has no damping in the dead zone, it was of interest to investigate whether the motion entered a very slow limit cycle mode crossing the entire dead zone or whether the trajectory entered a type of limit cycle around one edge of the dead zone.

To explore these possibilities several of the preceding simulations were repeated using a longer problem time. These results were not conclusive, but several of the test cases did recycle about one edge of the dead zone without ever crossing the dead zone.

No valid conclusions can be drawn at this point, especially in view of the fact that the simulation model was a much simpler system than any practical realization. It is clear, however, that the type of behavior observed is due to the sampled nature of the nonlinear system. One suspects that this oscillatory behavior can be changed substantially by altering the sampling period.

7. Conclusions

This report has considered the problem of estimating regions of boundedness for discrete-time dynamic systems. Based on Liapunov-functions, several methods were developed for this purpose. A technique based on simple quadratic Liapunov functions led to a number of possible variants, with various degrees of complexity and a wide range of numerical difficulty. An example by this method was performed and the estimate compared with one obtained by simulation. Tentative conclusions from this example are that Liapunov results may be good and that simulation results may be difficult to interpret and time-consuming to generate; more examples, however, will be required for a definitive judgment on the effectiveness of these methods.

The other Liapunov-based technique made use of the Lur'e-Postnikov quadratic Liapunov function and yields estimates of regions of absolute boundedness. These results contain new and useful information regarding the influence of the nonlinearity on the boundedness region; this new information is apparently obtained at the cost of greater analytical complexity. The implications of this complexity, however, cannot be judged until further experience is gained with a computer implementation of this technique.

It should be noted that this Lur'e-based technique is limited in its present form to a system containing a single nonlinearity, while the simple quadratic Liapunov technique is applicable to systems containing multiple nonlinearities.

Based on studies to this time, the Liapunov methods of this report remain potentially attractive compared to the simulation method. Further work would profitably be devoted toward

increasing experience with the application of these techniques to a specific system, and to the development of effective computer programs for this purpose.

APPENDIX

ON PRACTICAL STABILITY*

Ljubomir T. Grujić
Mechanical Engineering Department
University of Belgrade
Belgrade, Yugoslavia

ABSTRACT

In this paper, a class of nonlinear nonautonomous systems with multiple nonlinearities is considered. Sufficient conditions are developed for a type of practical stability with specified settling time. The conditions are independent of the actual form of nonlinear characteristics so that they can be interpreted as conditions for "absolute" practical stability. The stability test is reduced to verification of the Hurwitz property of a constant matrix. This makes the stability analysis of the considered class of nonlinear systems convenient for machine computations.

The proposed practical stability analysis is applied to a third-order system with several nonlinearities.

1. INTRODUCTION

This paper is concerned with a practical stability analysis of nonautonomous nonlinear dynamic systems which have a number of nonlinearities depending on several variables.

Important results in practical stability analysis over a finite time interval have been obtained by Weiss and Infante [1] and Weiss [2]. They derived necessary [2] and sufficient [1] conditions expressed in terms of real valued functions. In this work, as in reference [3], the function $V(x)= b^T|x|$ is proposed as a candidate for system Liapunov function. This function leads to algebraic conditions for testing *practical stability with a specified settling time*, which is defined over a prescribed (finite or infinite) time interval.

* The research reported herein was supported by the National Aeronautics and Space Administration under the Contract No. NAS-27799.

2. NOTATIONS

$A = (a_{ij})$, $n \times n$ constant matrix.

$b = (b_1\ b_2\ \dots\ b_n)^T$, constant positive vector.

$c = (c_1\ c_2\ \dots\ c_n)^T$, constant positive vector.

$v \in R^m$, $\mathcal{V} = \{z:||z|| \leq \gamma\}$, set of all allowed vector disturbances.

$f:R^n \times R^m \times T \to R^n$, $f = (f_1\ f_2\ \dots\ f_n)^T$

$g:R^n \times R^m \times T \to R^n$, $g = (g_1\ g_2\ \dots\ g_n)^T$

$H \subset R^{n^2}$, $H = \{A:\mathrm{Re}\ \lambda_i(A) < 0\ ,\ i = 1, 2, \dots, n\}$.

$H:R^n \times R^m \times T \to R^{n^2}$, $H = (h_{ij})$.

$N:R^n \to R^n$, $N = (N_1\ N_2\ \dots\ N_n)^T$.

$P_{(\cdot)} \subset R^n$, $P_{(\cdot)} = \{x:|x| \leq s^{(\cdot)}\}$, $(\cdot) = a, 1, f$, $P_f \subset P_1 \subset P_a$.

$P_\ell \subset P_f$, P_ℓ^i is the largest subset of P_f such that $P_\ell = \{x:V(x) \leq V_{MP_\ell^i} \leq V_{mP_\ell^b} < V_{MP_\ell^b} \leq V_{mP_L}\}$.

$P_L \subset P_a$, $P_L = P_a - P_\ell^i = \{x:x \in P_a \text{ and } x \notin P_\ell^i\}$.

$P_{(\cdot)}^b$ boundary of a closed set $P_{(\cdot)}$; $P_{(\cdot)}^i = P_{(\cdot)} - P_{(\cdot)}^b$.

R^i i-dimensional real vector space.

$s^{(\cdot)} = [s_1^{(\cdot)}\ s_2^{(\cdot)} \dots s_n^{(\cdot)}]^T > 0$, $(\cdot) = a, f, i$, prescribed constant positive vector.

$\operatorname{sgn} x = \operatorname{diag}(\operatorname{sgn} x_1\ \operatorname{sgn} x_2 \dots \operatorname{sgn} x_n)$.

$t \in R^1$, $-\infty < t_0 \le t < +\infty$.

τ: either $\tau \in R^1$ and $\tau > 0$, or $\tau = +\infty$.

$\tau_s \in R^1$, $\tau_s \in (0, \tau)$, system settling time.

$T \in R^1$, $T = (t: t_0 \le t < t_0 + \tau)$, $T_s = (t: t_0 + \tau_s \le t < t_0 + \tau)$.

$V: R^n \to R^1$, $V_{m(\cdot)} = \min_{(\cdot)} V(x)$, $V_{M(\cdot)} = \max_{(\cdot)} V(x)$. $\dot V(x)$ is the total time derivative of $V(x)$ along solutions of a system.

$x = (x_1\ x_2 \dots x_n)^T$, state of a system.

$x(t; x_0, t_0)$: $R^n \times T \to R^n$, motion of a system satisfying $x(t_0; x_0, t_0) = x_0$.

$z: R^n \times T \to R^m$, $z(x, t)$ is a disturbance vector.

δ_{ij} Kronecker delta.

$\varepsilon_i = (+1 \text{ or } -1) = \text{const.}$, $i = 1, 2, \dots, n$.

$\varepsilon = \operatorname{diag}(\varepsilon_1\ \varepsilon_2 \dots \varepsilon_n)$.

$\sigma: R^n \times R^m \times T \to R^n$, $\sigma = (\sigma_1\ \sigma_2 \dots \sigma_n)^T$.

$|x| \le s^{(\cdot)} \leftrightarrow |x_i| \le s_i^{(\cdot)}$, $i = 1, 2, \dots, n$.

$||(\cdot)|| = [(\cdot)^T(\cdot)]^{1/2}$.

3. PRACTICAL STABILITY WITH SPECIFIED SETTLING TIME

In this paper, we shall study a class of systems governed by the vector differential equation

$$\frac{dx}{dt} = g(x, z, t) , \qquad (1)$$

where $z = z(x, t) \in \mathcal{D}$ on $P_a \times T$. Motions $x(t; x_0, t_0)$ of system (1) are required to satisfy $x(t; x_0, t_0) \in P_a$, $\forall t \in T$, and $x(t; x_0, t_0) \in P_f$, $\forall t \in T_s$, whenever $x_0 \in P_i$, $z \in \mathcal{D}$. More precisely:

Definition: *System (1) is practically stable with the settling time τ_s if and only if $x_0 \in P_i$, $z \in \mathcal{D}$ imply:*

(i) $x(t; x_0, t_0) \in P_a$, $\forall t \in T$, *and*

(ii) $x(t; x_0, t_0) \in P_f$, $\forall t \in T_s$.

It is important to note the difference between the definition of contractive stability of reference [1] and the definition proposed above. The former is related to practical stability over a finite time interval and only the existence of a number τ_s is required. The latter is concerned with practical stability over a given time interval T , which may be either finite or infinite. Moreover, the number $\tau_s \in (0, \tau)$ is a specified positive number. In the sequel, $\tau = +\infty$.

Now we state:

Theorem 1: *Let $V(x) = b^T|x|$. System (1) is practically stable with the settling time τ_s if there exists a constant vector $b > 0$ such that the following conditions are satisfied*

(i) $b^T s^i \le \min_{j=1,2,\dots,n} \{b_j s_j^a\}$,

(ii) $\dot V(x) < 0$ *on* $P_L \times \mathcal{D} \times T$,

(iii) $\tau_s \ge [V_{mP_\ell^b} - V_{M(P_i - P_\ell^i)}]\, \dot V^{-1}_{MP_L} \times \mathcal{D} \times T$.

Theorem 1 is proved in Appendix 1. For a class of systems (1) satisfying assumptions defined in the sequel, a simple sufficient condition for the existence of a vector $b > 0$, which satisfies the condition (ii) of Theorem 1, is presented in Theorem 2.

Assumptions:

A.1 The vector function $g(x, z, t)$ may be written in the form $g(x, z, t) = H(x, z, t) \cdot f(x, z, t)$, i.e., system (1) may be described by equation

$$\frac{dx}{dt} = H(x, z, t)\, f(x, z, t) . \qquad (2)$$

A.2 $h_{ii}(x, z, t) < 0$ on $P_L \times \mathcal{D} \times T$, $i = 1, 2, \dots, n$. (If this assumption is satisfied only for $i = 1, 2, \dots, r < n$ then two additional assumptions should be satisfied [4]).

A.3 $|h_{ij}(x, z, t)| < +\infty$ on $P_a \times \mathcal{D} \times T$, $i, j = 1, 2, \dots, n$.

A.4 $f_i(x, z, t) \operatorname{sgn} x_i > 0$, $x_i \neq 0$, on $P_L \times \mathcal{D} \times T$, $i = 1, 2, \dots, n$.

Under the assumptions A.1-4 a matrix $A = (a_{ij})$ is defined by

$$a_{ij} = -\delta_{ij} \inf_{P_L \times D \times T} |h_{ij}(x, z, t)| + (1-\delta_{ij}) \sup_{P_L \times D \times T} |h_{ij}(x, z, t)| \quad , \quad (3)$$

and we have:

Theorem 2: *If* $A \in H$ *there exist infinite number of vectors* $b > 0$ *such that*

$\dot{V}(x) = b^T(\operatorname{sgn} x)\dot{x} \le |f^T(x, z, t)|A^T b < 0$ *on* $P_L \times D \times T$.

Theorem 2 is proved in Appendix 2.

The following procedure for an analysis of practical stability with specified settling time results from the previous theorems. A matrix function $H(x, z, t)$ and a vector function $f(x, z, t)$ should be selected to satisfy the assumptions A.1-4. Knowing $H(x, z, t)$ and $f(x, z, t)$ a matrix $A = (a_{ij})$ has to be determined according to Equation (3). The procedure may be continued only if $A \in H$, which guarantees (Theorem 2) the existence of infinite number of vectors $b > 0$ such that the condition (ii) of Theorem 1 is satisfied. A vector $b > 0$ should be chosen to satisfy the condition (i) of Theorem 1 and the inequality

$$A^T b < 0 \quad . \quad (4)$$

Provided that such a vector $b > 0$ has been determined, the condition (iii) of the same theorem has to be tested.

4. EXAMPLE

The outlined procedure for analysis of practical stability with specified settling time is now applied to system (1), where

$$g(x, z, t) = \begin{pmatrix} -0.2 & 0 & 0 \\ 0 & -1.0 & 2.0 \\ 0 & 0 & -5.0 \end{pmatrix} \begin{pmatrix} x_1 \\ x_2 \\ x_3 \end{pmatrix} + \begin{pmatrix} -0.2 & 0 & 0 & 0 \\ 0 & -20 & 0 & 0 \\ 0 & 0 & 2 & -100 \end{pmatrix} \begin{pmatrix} N_1(\sigma_1) \\ N_2(\sigma_2) \\ N_3(\sigma_3, \dot{\sigma}_3) \\ N_4(\sigma_4) \end{pmatrix},$$

$$\begin{pmatrix} \sigma_1 \\ \sigma_2 \\ \sigma_3 \\ \sigma_4 \end{pmatrix} = \begin{pmatrix} 0.5 & 0.5 & 0 \\ 0 & 1 & 0 \\ 0 & 1 & 0 \\ 2.5 \sin 3t & 7^{-1}x_3 & 10^{-3}|x_1| \end{pmatrix} \begin{pmatrix} x_1 \\ x_2 \\ x_3 \end{pmatrix},$$

$$N_1(\sigma_1) = \begin{cases} 69 & , \ \sigma_1 \ge 3.45 \\ \frac{138}{7.5}\sigma_1 & , \ |\sigma_1| \le 3.45 \\ -69 & , \ \sigma_1 \le -3.45 \end{cases}, \quad N_2(\sigma_2) = 60 \operatorname{sgn} \sigma_2,$$

$$N_3(\sigma_3, \dot{\sigma}_3) = \begin{cases} 10 \operatorname{sgn} \sigma_3 & \begin{cases} |\sigma_3| > 4, \text{ or} \\ |\sigma_3| > 2, \ \sigma_3\dot{\sigma}_3 < 0 \end{cases} \\ 0 & \begin{cases} |\sigma_3| < 4, \ \sigma_3\dot{\sigma}_3 > 0 \\ |\sigma_3| < 2 \end{cases} \end{cases},$$

$$N_4(\sigma_4) = \begin{cases} 12 \operatorname{sgn} \sigma_4 & , \ |\sigma_4| \le 6 \\ 3(|\sigma_4| - 2)\operatorname{sgn} \sigma_4 & , \ 2 \le |\sigma_4| \le 6 \\ 0 & , \ |\sigma_4| \le 2 \end{cases},$$

$$s^a = \begin{pmatrix} 16 \\ 30 \\ 70 \end{pmatrix}, \ s^1 = \begin{pmatrix} 4 \\ 5 \\ 10 \end{pmatrix}, \ s^f = \begin{pmatrix} 1.0 \\ 0.5 \\ 1.0 \end{pmatrix}, \ \tau_s = 12 \text{ sec.}$$

In this example, $f(x, z, t)$ and $H(x, z, t)$ are selected as $f(x, z, t) = x$,

$$H(x, z, t) = \begin{pmatrix} -0.2 - 0.1\frac{N_1(\sigma_1)}{\sigma_1} & ; 0 & ; -250\frac{N_4(\sigma_4)}{\sigma_4}\sin 3t \\ -0.1\frac{N_1(\sigma_1)}{\sigma_1} & -1 - 20\frac{N_2(\sigma_2)}{\sigma_2} & ; 2\frac{N_3(\sigma_3, \dot{\sigma}_3)}{\sigma_3} - 7^{-1}100\frac{N_4(\sigma_4)}{\sigma_4}x_3 \\ 0 & ; 2 & ; -0.5 - 0.1\frac{N_4(\sigma_4)}{\sigma_4}|x_1| \end{pmatrix}^T$$

The above selection of functions $f(x, z, t)$ and $H(x, z, t)$ is made in order to satisfy assumptions A.1-4. According to Equation (3), we get

$$A = \begin{pmatrix} -0.5 & 2 & 0 \\ 0 & -41 & 2 \\ 5 & 30 & -5 \end{pmatrix} \in H \ .$$

The vector b is chosen to be $b = (101 \quad 22 \quad 10)^T$, such that 1st and 2nd condition (Theorem 2) of Theorem 1 are satisfied.

The following numbers are calculated for the selected vector b as

$$V_{M(P_1 - P_2^1)} = 614 \quad V_{mP_2^0} = 10 \quad \dot{V}_{MP_L} = -50.5 \ .$$

Therefore,

$[V_{mP_\ell^b} - V_{M(P_1-P_\ell^i)}] \hat{V}^{-1}_{MP_L \times \mathcal{V} \times T} < 12 = \tau_s$.

Hence, the conditions (i-iii) of Theorem 1 are satisfied, and the analyzed system is practically stable with the settling time 12 sec.

5. CONCLUSIONS

In this paper, a definition of practical stability with specified settling time is proposed. The outlined analysis provides information about quality of the forced system dynamic behavior over a prescribed time interval, which may be finite or infinite, and about a value of the system settling time.

An analysis of the proposed type of practical stability has been carried out for a broad class of nonlinear nonautonomous dynamic systems. The class of systems is defined by some general requirements and is limited neither by the order of system nor by the form of nonlinearities. The latter fact shows that the proposed procedure enables an investigation of "absolute" practical stability. The stability test is reduced to verification of the Hurwitz property of a constant matrix and to a choice of a positive vector to satisfy given inequalities. In complex situations procedure may require machine computations.

ACKNOWLEDGEMENT

The author is indebted to Professor Dragoslav D. Šiljak, Electrical Engineering Department, University of Santa Clara, Santa Clara, California, for his useful comments on this paper.

APPENDIX 1

If $b > 0$ then the following is true:

$V(x) = b^T|x| > 0$, $\forall x \neq 0$; $V(x) \to \infty$ for $||x|| \to \infty$,

and since $\dot{V}(x) < 0$ on $P_L \times \mathcal{V} \times T$, according to condition (ii) of Theorem 1, then $V(x)$ is a system Liapunov function on $P_L \times \mathcal{V} \times T$. From the same condition it follows that, for $\forall t \in T$,

$V[x(t; x_0, t_0)] \leq V(x_0)$. From condition (i) of Theorem 1, and from the previous result, one obtains

$$V[x(t; x_0, t_0)] \leq V(x_0) \leq b^T s^1 \leq \min_{j=1,2,\ldots,n} (b_j s_j^a), \quad \text{(A-1)}$$

on $P_1 \times \mathcal{V} \times T$.

Therefore, $|x_j(t; x_0, t_0)| \leq s_j^a$, on $P_1 \times \mathcal{V} \times T$, $j = 1, 2, \ldots, n$, i.e.

$$x(t; x_0, t_0) \in P_a \text{ , on } P_1 \times \mathcal{V} \times T \text{ .}$$

Furthermore

$$\dot{V}(x)\big|_{P_L} \leq \dot{V}_{MP_L} < 0 \text{ .} \qquad \text{(A-2)}$$

Integrating the last expression in (A-2) from t_0 to t , we get

$$V(x)\big|_{P_L} - V(x_0)\big|_{P_1 - P_\ell^i} \leq V_{MP_L}(t - t_0) < 0. \qquad \text{(A-3)}$$

Since P_ℓ is defined as the largest of P_f such that

$$V(x)\big|_{P_\ell^i} \leq V_{MP_\ell^i} \leq V_{mP_\ell^b} < V_{MP_\ell^b} \leq V_{mP_L} \text{ ,} \qquad \text{(A-4)}$$

then from (A-3) it follows that

$$V_{M(P_1-P_\ell^i)} - V_{mP^b} \geq -\dot{V}_{MP_L}(t - t_0) \text{ ,} \qquad \text{(A-5)}$$

or

$$t\big|_{x(t; x_0, t_0)\ P_\ell} - t_0 = \tau_{sa} \leq [V_{mP_\ell^b} - V_{M(P_1-P_\ell^i)}] \hat{V}^{-1}_{MP_L} \leq \tau_s \text{ ,} \qquad \text{(A-6)}$$

where $\tau_{sa} = (t\big|_{x(t; x_0, t_0)\ P_\ell} - t_0)$ is the actual settling time, which is evidently less than the given τ_s . From (A-2) and (A-4) it also follows that $|x_j(t; x_0, t_0)| \leq s_j^f$ on $P_1 \times \mathcal{V} \times T_s$, $j = 1, 2, \ldots, n$, i.e.

$$x(t; x_0, t_0) \in P_f \text{ on } P_1 \times \mathcal{V} \times T_s \text{ .}$$

This proves Theorem 1.

APPENDIX 2

The proof of Theorem 2 is based on Persidskii's lemma in [3] and the following assumption:

Assumption (A-A): The elements of a certain basis (e_i) and the coefficients of the matrix $A = (a_{ij})$ are related by

$$a_{ij} e_i e_j \geq 0 \text{ , } i \neq j \text{ , } i, j = 1, 2, \ldots, n. \qquad \text{(A-1)}$$

Lemma [3]: Assume the coefficients of the matrix $A = (a_{ij})$ are such that the inequalities (A-1) are satisfied for a certain basis (e_i). Then in order for all roots of the secular equation

$$\det(A - \lambda I) = 0$$

to have negative real parts it is necessary and sufficient if for any positive vector c *a vector* b *determined from the equation*

$$A^T \epsilon b = -\epsilon c \qquad \text{(A-2)}$$

is positive.

Let the elements a_{ij} of the matrix A be defined by

$$a_{ij} = -\delta_{ij} \inf_{P_L \times D \times T} |h_{ij}(x, z, t)| + (1-\delta_{ij}) \sup_{P_L \times D \times T} |h_{ij}(x, z, t)| , \qquad \text{(A-3)}$$

provided that $h_{ij}(x, z, t)$ satisfy the assumptions A.1-3, $i, j = 1, 2, \ldots, n$. It can be easily varified that all elements a_{ij}, Equation (A-3), satisfy Assumption (A-A) whenever ϵ is chosen to be the indentity matrix, i.e.

$$\epsilon = \text{diag}\{1 \;\; 1 \;\; \ldots \;\; 1\} = I . \qquad \text{(A-4)}$$

Now, we proceed to prove Theorem 2. For system (1) satisfying the assumptions A.1-4 and for

$$V(x) = b^T|x| = b^T (\text{sgn } x)x ,$$

$$\dot{V}(x) = b^T (\text{sgn } x)\dot{x} = b^T (\text{sgn } x) H(x, z, t) f(x,z,t) = f^T(x, z, t) H^T(x, z, t)(\text{sgn } x)b . \qquad \text{(A-5)}$$

Using assumption A.4 and Equations (A-3) we obtain the following relation for $\dot{V}(x)$

$$\dot{V}(x) = |f^T(x, z, t)|(\text{sgn } x) H^T(x, z, t)(\text{sgn } x)b \leq \leq |f^T(x, z, t)|A^T b \quad \text{on} \quad P_L \times D \times T . \qquad \text{(A-6)}$$

If $A \in H$, according to the Lemma [3] and Equations (A-3), (A-4), for any $c > 0$, there exists a vector $b > 0$ such that

$$A^T b = -c < 0 . \qquad \text{(A-7)}$$

From Equations (A-6), (A-7) we conclude that

$$\dot{V}(x) \leq -|f^T(x, z, t)|c < 0 \quad \text{on} \quad P_L \times D \times T$$

and since $c > 0$ is an arbitrary positive vector, the proof of Theorem 2 is complete.

REFERENCES

[1] Weiss, L. and Infante, E. F., "Finite Time Stability Under Perturbing Forces and on Product Spaces", IEEE Trans., Vol. AC-12, No. 1, 1967, pp. 54-59.

[2] Weiss, L., "Converse Theorems for Finite Time Stability", Proceedings of the First Asilomar Conference on Circuits and Systems, Asilomar, California, November 1-3, 1967, pp. 1006-1014.

[3] Persidskii, L. K., "Problem of Absolute Stability", (in Russian), Avtomatika i Telemekhanika, No. 12, December 1969, pp. 5-11.

[4] Grujić, Lj. T., "Automatic Control System Synthesis of Rigid Body Motion Through a Fluid", M.S. Thesis, (in Serbo-Croatian), Electrical Engineering Department, University of Belgrade, Belgrade, Yugoslavia, October, 1970.

References

[1] LaSalle, J. and S. Lefschetz, Stability by Liapunov's Direct Method, Academic Press, N.Y., 1961.

[2] Johnson, G. W., "Upper Bound Quantization in Digital Control Systems via the Direct Method of Liapunov", IEEE Trans. Automatic Control, Vol. AC-10, No. 4, October 1965, pp. 439-448.

[3] Lack, G.N.T., "Comments on Upper Bound on Dynamic Quantization Error in Digital Control Systems via the Direct Method of Liapunov", IEEE Trans. Automatic Control, Vol. AC-11, April 1966, pp. 331-333.

[4] Parker, S. R. and S. F. Hess, "Limit-Cycle Oscillations in Digital Filters", IEEE Trans. Circuit Theory, Vol. CT-18, No. 6, November 1971, pp. 687-697.

[5] Weissenberger, S., "Extended Boundedness Concept for the Problem of Lur'e", Electronics Letters, Vol. 4, No. 22, November 1968, p. 489.

[6] Siljak, D. D. and S. Weissenberger, "Regions of Exponential Ultimate Boundedness for the Problem of Lur'e", Regelungstechnik und Process-Datenverarbeitung, Vol. 18, No. 2, October 1970, pp. 69-71.

[7] Willems, J. L., Stability Theory of Dynamical Systems, Nelson, London, 1970.

[8] Barnett, S. and C. Storey, Matrix Methods in Stability Theory, Nelson, London, 1970.

[9] Rodden, J. J., "Numerical Applications of Liapunov Stability Theory", Joint Automatic Control Conference, Stanford, California, 1964, pp. 261-268.

[10] Nelson, W., Nonlinear Control Systems Analysis by Liapunov's Direct Method, M.S. Thesis, University of Santa Clara, Santa Clara, Calif., 1967.

[11] Geiss, G., et al., An Algorithm for Liapunov Stability Analysis of Complex Nonlinear Systems with Application to the Orbiting Astronomical Observatory, NASA CR-1729, 1971.

[12] Weissenberger, S., "Stability Boundary Approximations for Relay-Control Systems via a Steepest-Ascent Construction of Liapunov Functions", Trans. ASME, J. Basic Engineering, Vol. 88, No. 2, June 1966, pp. 419-428.

[13] Tsypkin, Ya Z., "On Stability in the Large of Nonlinear Discrete Automatic Systems" (in Russian), Dokl. Akad. Nauk SSSR, Vol. 145, 1962, pp. 52-55.

[14] Siljak, D. D. and C. K. Sun, "Absolute Stability Test for Discrete Systems", Electronics Letters, Vol. 5, No. 11, May 1969, p. 236.

[15] Szegö, G. and R. Kalman, "Sur la stabilité absolute d'un système d'équations aux différences finies", Compt. rend. Acad. Sci., Paris, Vol. 257, July 1963, pp. 388-390.

[16] Siljak, D. D. and C. K. Sun, "Exponential Absolute Stability of Discrete Systems", ZAMM, Vol. 51, No. 4, July 1971, pp. 271-275.

[17] Seltzer, S. M., "Sampled-Data Control System Design in the Parameter Plane", Proceedings, 8th Allerton Conference, Oct. 1970.